CHAPTER IV

RESULTS AND DISCUSSION

1. Preliminary bioactivity screening

During the course of screening for bioactive metabolites from actinomycetes, the crude ethyl acetate extract of the YM fermentation broth of actinomycete strains showed interesting antimicrobial activity and bioactivity (Tables 7 and 8). The crude extract of PNK1-3 exhibited interesting antimicrobial activity against *C. albicans* ATCC 10231, *M. luteus* ATCC 9341 and *S. aureus* ATCC 25923 with 18.5 mm, 20.5 mm and 18.0 mm, respectively. All isolates could inhibit growth of *M. luteus* ATCC 93410.

The incidences of tuberculosis and malaria have rapidly increased worldwide, particularly among those associated with HIV infection. WHO is estimated that more than 300 million cases are infected with malaria and 1 million deaths of children each year (Corbett. *et. al* 2002). As a result of biological activity, the crude extract of PNK1-3 showed cytotoxicity against KB cells and BC cells with respective IC_{50} 17.9 and 0.14 μg/ml, and this led us to investigate bioactive constituents of this bacteria.

Table 7 Antimicrobial activity of strains (1mg/6mm disc)

Strains	Inhitbition zone (mm)				
	S. aureus ATCC 25923	*B. subtilis* ATCC 6633	*M. luteus* ATCC 9341	*E. coli* ATCC 25922	*C. albicans* ATCC 10231
PNK1-3	18.0	14.2	20.5	10.0	18.5
PNK1-5	17.03	12.7	18.2	10.5	17.4
KN-6	12.5	14.5	13.8	-	10.0
TT2-9	15.0	-	-	-	-
FLM-2	-	-	14.5	-	-
MA-1	10.4	12.4	13.8	-	7.5
MA-2	11.0	13.3	15.8	-	9.6
JSM1-1	10.0	11.0	13.0	-	8.0
JSM1-3	10.8	10.2	11.0	-	8.9
MC5-1	11.3	11.5	12.0	-	-
MC7-1	11.9	10.5	13.0	-	-
R1-1	10.5	11.8	12.3	-	-

Table 8 Biological activity of strains

Compound	Anticandida[a] activity MIC (μg/mL)	Antimalarial[a] activity IC_{50}(μg/mL)	Antimycobacterial[b] activity MIC (μg/mL)	Cytotoxicity IC_{50} (μg/mL)*	
				KB cell[c]	BC cell[d]
PNK1-3	34.15	30	50	17.9	0.14
KN-6	Inactive	3.3	100	14.5	2.7
MA-1	Inactive	Inactive	Inactive	Inactive	Inactive
MA-2	Inactive	Inactive	Inactive	Inactive	Inactive
JSM1-1	Inactive	Inactive	200	Inactive	Inactive
JSM1-3	Inactive	Inactive	200	Inactive	Inactive
MC5-1	Inactive	Inactive	-	Inactive	Inactive
MC7-1	Inactive	Inactive	-	Inactive	Inactive
R1-1	Inactive	Inactive	200	Inactive	Inactive

2. Morphological and cultural characteristics of the strains

The morphological characteristics and cultural characteristics of twelve isolates (Table 9) on YMA medium at 30 °C (14 days) showed the presence of five isolates of the family *Streptomycetaceae* possessed aerial mycelium and powdery colonies. The isolates, PNK1-3 and PNK1-5 showed spiral spore chain and three isolates, TT2-9, KN-6 and FLM-2 were rectiflexibles spore chain. PNK1-3, PNK1-5 and FLM-2 were white mycelial pigment, TT2-9 as brownish white, and KN-6 as purple. All isolates grew well on YMA and oat meal agar. The vegetative mycelium of the first selected strain PNK1-3 on YMA mycelium was initially white and turned into dark during incubation for 21 days. PNK1-3 showed unbranched aerial hyphae, spiral chains of cylindrical spores with rugose ornamentation (Figure 1). The second selected strain is FLM-2 on YMA mycelium was initially white and turned to silver gray and no soluble pigment was produced. FLM-2 produced aerial mycelial that consisted of long straight chains of 20 or more spores with smooth surfaces (Figure 2).

Seven isolates showed mucoid colonies with single spore on short sporophore of the vegetative mycelium, but no aerial hyphae. They were identified as *Micromonospora*. On the results of phenotypic characteristics of strains (Table 11) seven strains *Micromonospora* could be classified into 3 groups. Group I was MA-1 and MA-2, group II as JSM1-1 and JSM1-3, group III as MC5-1, MC7-1 and R1-1.They produced well-developed and branched substrate hyphae on yeast extract-malt extract medium. Spores of them were borne singly on the substrate hyphae

having approximately diameter of 0.5-0.6 μm. The spores were rough, nodular, and smooth on the surface and non-motile. The colors of the substrate mycelium were vivid orange ant tuned to brownish black to black after sporulation.

Table 9. Cultural characteristics of the strains

Isolate No.	Media	Growth	Color of upper surface	Color of reverse surface	Soluble pigment
PNK1-3	YM	abundant	blackish gray to white	light grayish yellow, pale yellow	pale yellow
	OM	abundant	black	grayish yellow	-
	IS	good	grayish white	pale yellow	-
	TA	abundant	light gray	grayish yellow	brown
	GlyA	moderate	grayish yellow	brown	-
	GluA	moderate	yellowish white	pale yellow	-
	NA	moderate	blackish gray to white	brownish black	-
	PIA	good	white	brown	-
PNK1-5	YM	abundant	blackish gray to white	light grayish yellow, pale yellow	pale yellow
	OM	abundant	black	grayish yellow	-
	IS	good	grayish white	pale yellow	-
	T.A.	abundant	light gray	grayish yellow	brown
	GlyA	moderate	grayish yellow	brown	-
	GluA.	moderate	yellowish white	pale yellow	-
	NA	moderate	blackish gray to white	brownish black	-
	PIA	good	white	brown	-
KN-6	YM	abundant	deep purplish red	deep purplish red	yellow
	OM	abundant	dull red purple	dull red purple	-
	IS	good	purplish rose	deep purplish red	-
	TA	moderate	deep purplish red	deep purplish red	-
	GlyA	poor	purplish rose	vivid red purple	-
	GluA	moderate	pink to red	vivid purple	-
	NA	moderate	dull red purple	purple	-
	PIA	poor	pink to red	purple	-

Table 9. Cultural characteristics of the strains (continued)

Isolate No.	Media	Growth	Color of upper surface	Color of reverse surface	Soluble pigment
	YM	abundant	white, pale grey	yellowish brown	pale yellow
	OM	abundant	grey to dark grey	grayish brown, dark brown	-
FLM-2	IS	good	grey	yellowish grey	-
	TA	good	dark yellowish brown	yellowish brown	-
	GlyA	moderate	grey	brownish gold	-
	GluA	moderate	grey to brownish black	brown	-
	NA	abundant	white to grey	white to grey	-
	PIA	moderate	brownish black	yellowish brown	-
	YM	abundant	Light brownish white	yellowish brown	pale yellow
	OM	abundant	dark grey	yellowish brown	-
	IS	good	brownish gold	yellowish brown	
TT2-9	TA	good	brownish white	yellowish brown	-
	GlyA	moderate	brownish white	brownish gold	-
	GluA	moderate	grey to brownish black	brown	-
	NA	abundant	dark grey	yellowish brown	-
	PIA	moderate	brownish black	yellowish brown	-
	YM	abundant	brownish black	deep orange	yellow
	OM	abundant	dark brownish black	vivid orange	-
	IS	good	orange	vivid orange	-
MA-1	TA	moderate	dark yellowish brown	yellowish brown	-
	GlyA	poor	dark brownish black	light yellowish brown	-
	GluA	poor	brownish black	deep orange	-
	NA	moderate	brownish black to black	vivid orange	-
	PIA	poor	dark yellowish brown to black	deep orange	-

Table 9. *Cultural characteristics of the strains (continued)*

Isolate No.	Media	Growth	Color of upper surface	Color of reverse surface	Soluble pigment
MA-2	YM	abundant	orange to brown to black	deep orange	yellow
	OM	abundant	dark brownish black	vivid orange	-
	IS	good	brownish black	vivid orange	-
	TA	moderate	dark yellowish brown	yellowish brown	-
	GlyA	poor	light yellowish brown	light yellowish brown	-
	GluA	poor	brownish black	deep orange	-
	NA	moderate	brownish black to black	vivid orange	-
	PIA	poor	dark yellowish brown to black	deep orange	-
JSM1-1	YM	abundant	brite orange	dull orange	pale yellow
	OM	good	brown, cinnamon	light brown	-
	IS	poor	light ivory, light wheat	yellowish white	-
	TA	poor	yellowish white to white	yellowish white	pale brown
	GlyA	poor	yellowish white	yellowish white	-
	GluA	poor	yellowish white	yellowish white	-
	NA	moderate	light brown	brown	-
	PIA	moderate	orange	orange	-
JSM1-3	YM	abundant	brownish Black	dull orange	pale yellow
	OM	abundant	yellowish brown, cinnamon	light brown	-
	IS	poor	light brown	yellowish white	-
	TA	poor	yellowish white	yellowish white	brown
	GlyA	poor	yellowish white	yellowish white	-
	GluA	poor	white	yellowish white	-
	NA	moderate	light brown	brown, cinnamon	-
	PIA	moderate	orange	orange	-

Table 9. Cultural characteristics of the strains (continued)

Isolate No.	Media	Growth	Color of upper surface	Color of reverse surface	Soluble pigment
MC5-1	YM	abundant	brownish black to black	vivid orange	pale brown
	OM	abundant	brownish black	vivid orange	-
	IS	good	grayish black	orange	-
	TA	moderate	brownish black	grayish white	brown
	GlyA	good	gray	grayish white	-
	GluA	moderate	pale white	pale orange	-
	NA	moderate	light brown	brown	-
	PIA	moderate	brown	dark yellowish, orange	-
MC7-1	YM	abundant	brownish black to black	vivid orange	pale brown
	OM	abundant	brownish black	vivid orange	-
	IS	abundant	black	orange	-
	TA	moderate	black	grayish white	brown
	GlyA	good	gray	grayish white	-
	GluA	moderate	pale white	grayish white	-
	NA	moderate	light brown	brown	-
	PIA	moderate	brown	dark yellowish orange	-
R1-1	YM	abundant	brownish black to black	vivid orange	pale brown
	OM	abundant	dark brownish black	vivid orange	-
	IS	good	brown	orange	-
	TA	moderate	black	grayish white	brown
	GlyA	moderate	black	grayish white	-
	GluA	moderate	gray, pale orange to brown	pale orange	-
	NA	moderate	dark brown	brown	-
	PIA	moderate	orange	dark yellowish orange	-

YM, Yeast extract-malt extract; OM, Oatmeal; IS, Inorganic salts-starch agar; TA, Tyrosine agar ; GlyA, Glycerolasparagine agar; GluA, Glucose-asparagine agar; NA, Nutrient agar; PIA, Peptone-yeast extract iron agar

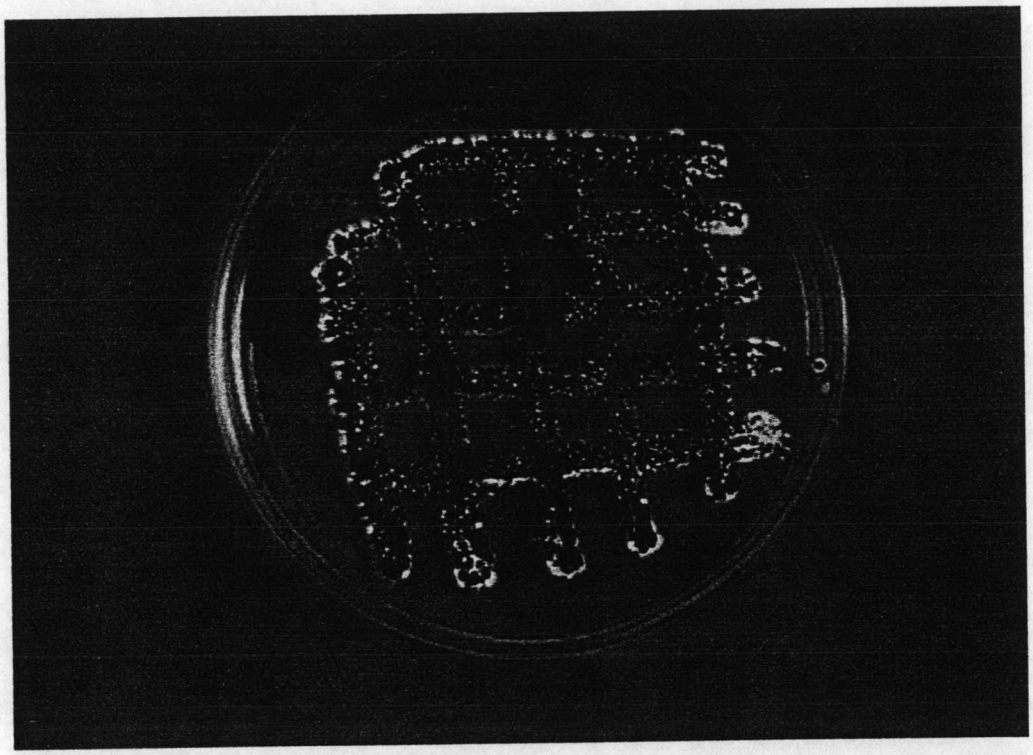

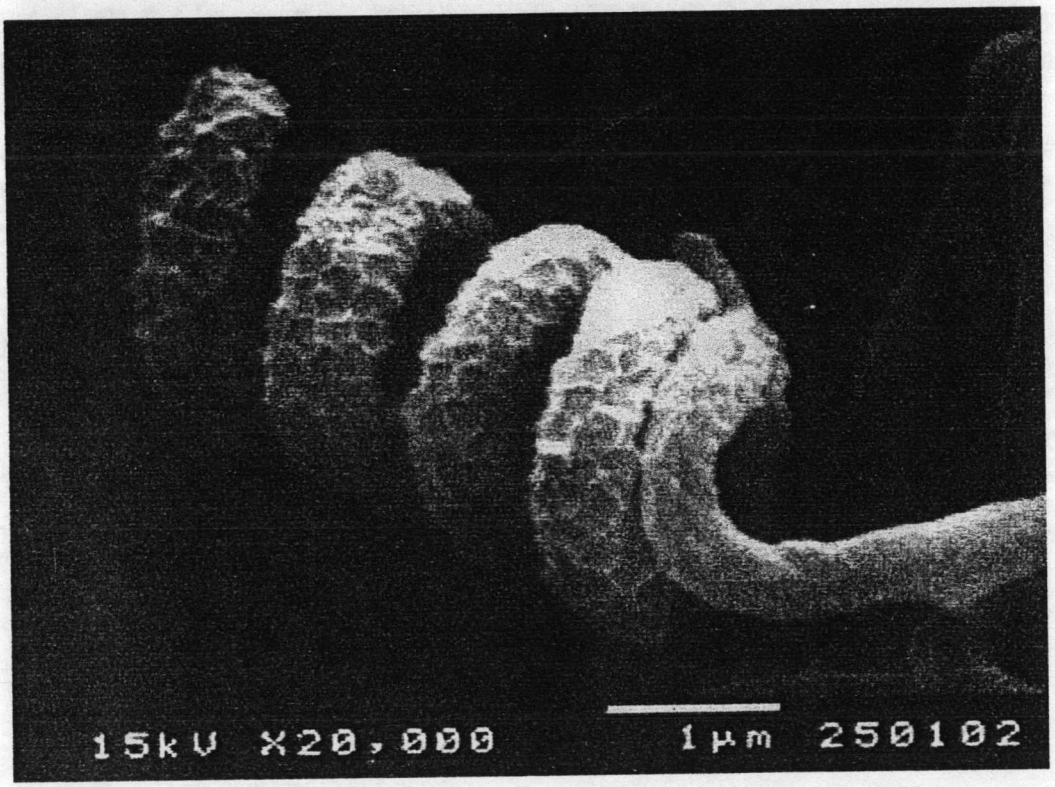

Figure 1. The colonial appearance and scanning electron micrograph of PNK1-3 on YMA medium (21 days)

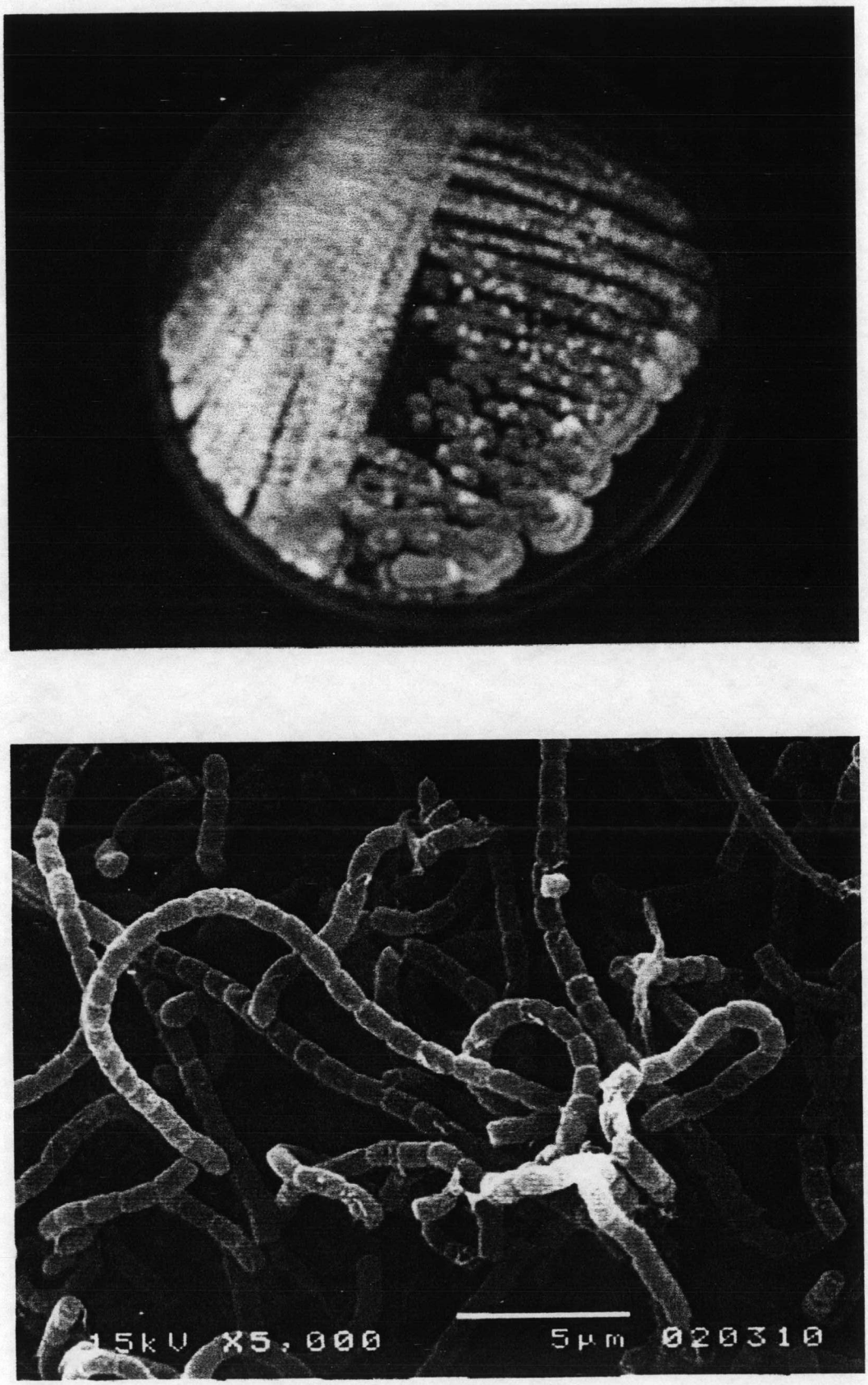

Figure 2. The colonial appearance and scanning electron micrograph of FLM-2 on YMA medium (21 days)

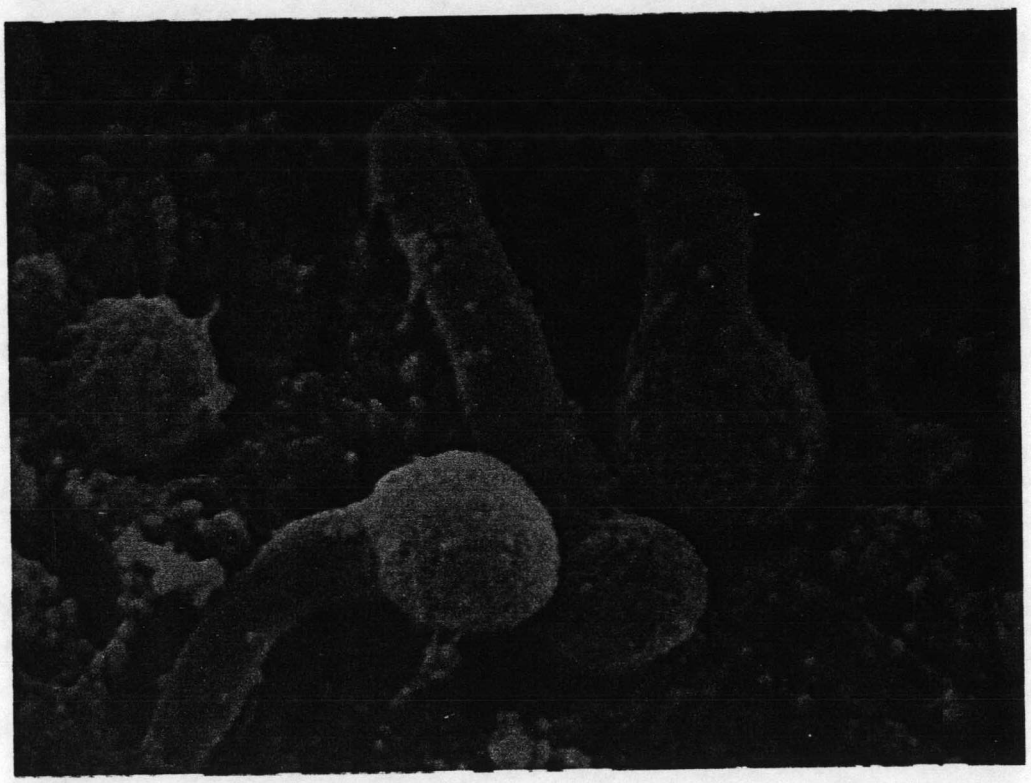

Figure 3. The colonial appearance and scanning electron micrograph of MA-2 on YMA medium (21 days)

Figure 4. The colonial appearance and scanning electron micrograph of JSM1-1 on YMA medium (21 days)

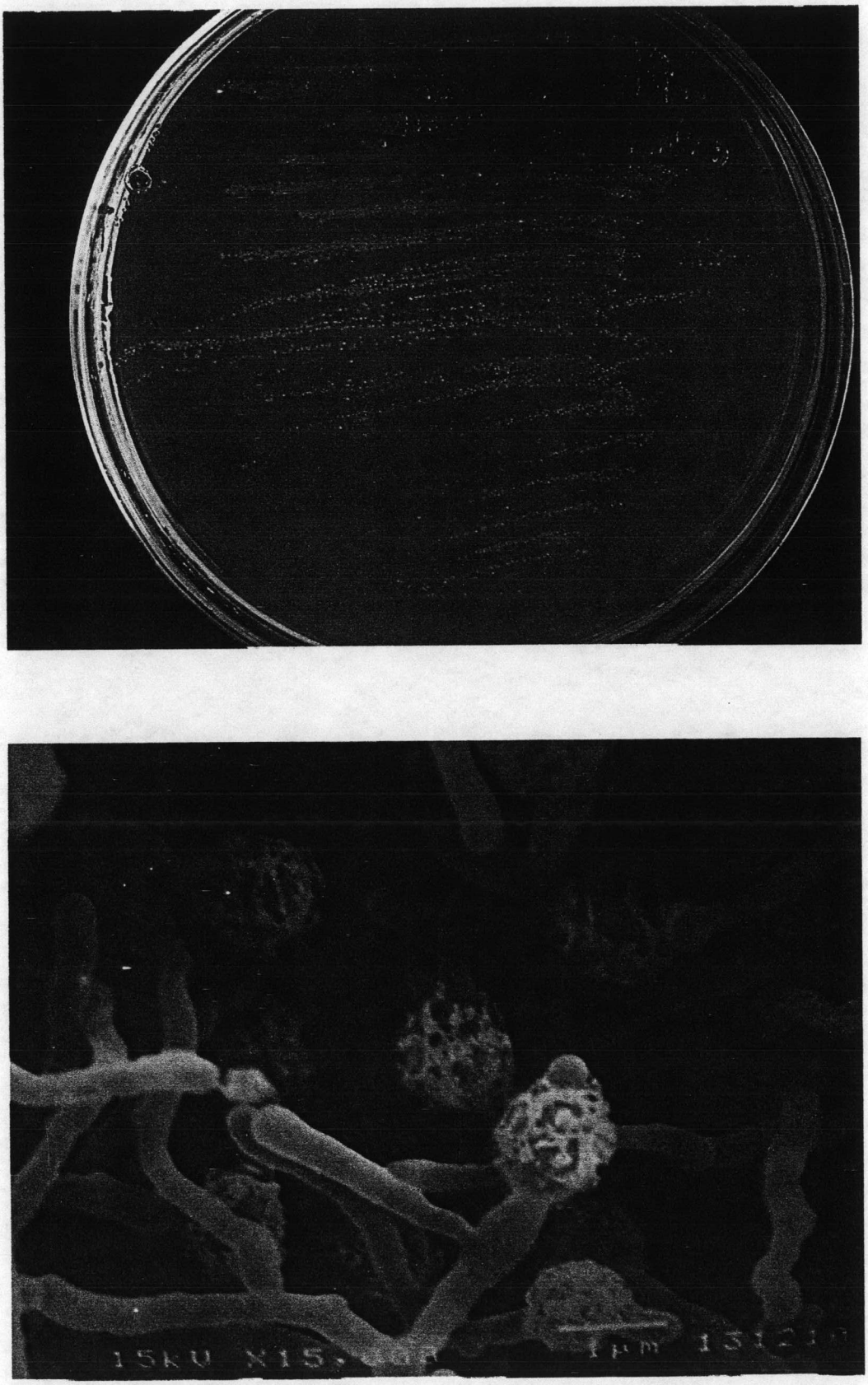

Figure 5. The colonial appearance and scanning electron micrograph of MC5-1 on YMA medium (21 days)

The morphological characteristics and phylogenetic tree of twelve strains were consistent with their identify in the family *Streptomycetaceae* 5 strains, and 7 strains *Micromonosporaceae* (Shirling and Gottlieb, 1976; Zhang *et al*, 1997; Kawamoto, 1989). PNK1-3 was represented of *Streptomyces* for studying physiological and biochemical characteristic since it showed significant antimicrobial and cytotoxic activity. The colonies of FLM-2 exhibited a *Streptomyces* liked. The colonial appearance and scanning electron micrograph of representative strains, PNK1-3, FLM-2, MA-2^T, JSM1-1^T, and MC5-1^T are shown in Figures 1-5. The cultural characteristics of all strains are summarized in Table 9.

3. Physiological and Biochemical Characteristics

PNK1-3, FLM-2 and 7 strains of *Micromonospora* shared many phenotypic and biochemical properties. All selected strains could hydrolyzed skim milk and starch. They could grow at pH 5-9, 3-6% NaCl (but most strains could grow in 3-4% NaCl). The suitable temperature range for growth was 25-30°C. All selected isolates showed antimicrobial activity. Variable characteristics and utilization of carbon sources are shown in Table 10.

PNK1-3 grew well at pH 6-8, the lower and the upper temperature limits for growth were 17-40 °C. PNK1-3 exhibited good growth in most media, positive for hydrolysis of starch, peptonization and coagulation of milk, gelatin liquefaction and nitrate reduction. PNK1-3 could grow on 4% NaCl containing agar. The secondary metabolites exhibited interesting bioactivities; antifungal, cytotoxicity against KB and BC cells.

FLM-2 grew well on ISP media and within the pH range 5.0-8.0. Temperature range for growth was 15-40 °C well optimum 25-30 °C. FLM-2 could hydrolysis of starch, peptonization and coagulation of milk, but not nitrate reduction and gelatin lique faction. FLM-2 could grow on 3 % NaCl. In addition, the secondary metabolites of FLM-2 inhibited growth of *Micrococcus luteus* ATCC 93410.

Micromonospora group I contained two isolates, including MA-1 and MA-2^T. They were positive for hydrolysis of starch, peptonization and coagulation of milk, but negative for reduction of nitrate. Well growth was observed between 25-30 °C, the lower and the upper temperature limits for growth were 10-45 °C. No growth was observed above 45 °C. The minimum pH and maximum NaCl for growth were pH 5 and 3 % NaCl.

Micromonospora group II contained two isolates, including JSM1-1^T and JSM1-3. They were positive for hydrolysis of starch, peptonization and coagulation of milk, but negative nitrate

reduction. Well growth was observed 3% NaCl and between 25-30 °C. The maximum temperature for growth of strains was at 45 °C. The minimum pH for growth was 5. They could grow on 7% NaCl. Their secondary metabolites inhibited growth of *Bacillus subtilis* ATCC 6633 and *Micrococcus luteus* ATCC 93410.

Micromonospora group III contained three isolates including MC5-1^T, MC7-1, and R1-1. They showed positive results for hydrolysis of starch, peptonization and coagulation of milk, but negative for reduction of nitrate. Well growth was observed between 25-30 °C. R1-1 could grow at 10-45 °C. No growth was observed above 45 °C. The minimum pH for growth was 4. The maximum NaCl concentration for growth was 4%.

Table 10 Carbon Utilization of the strains

Carbon sources	Isolates								
	PNK1-3	FLM-2	MA-1	MA-2	JSM1-1	JSM 1-3	MC5-1	MC7-1	R1-1
Utilization of									
D-Manitol	+	-	+	+	w	w	-	-	-
D-Ribose	+	w	w	w	+	+	-	-	-
L-Rhamnose	+	+	w	w	-	-	-	-	-
D-Melibiose	+	+	+	+	+	+	+	+	+
D-Raffinose	+	-	+	+	+	+	w	w	w
Glycerol	w	-	-	-	w	w	w	w	w
Salicin	w	w	+	+	-	-	+	+	+
Lactose	+	+	w	w	-	-	+	+	+
D-Galactose	+	+	+	+	+	+	+	+	+
L-Arabinose	-	+	+	+	+	w	+	+	+
D-Fructose	+	w	+	+	+	+	+	+	+
D-Xylose	+	+	+	+	+	+	+	+	+

Table 11 Physiological and biochemical characteristics of the strains

Isolate no.	Growth at (°C)							pH tolerance					NaCl tolerance (%)					Skim milk		Gelatin liquefaction	Nitrate reduction	Starch hydrolysis	Antimicrobial activies
	10	15	20	25	37	40	45	4	4.5	5	6	8	1	3	4	5	7	Peptonization	Coagulation				
PNK1-3	-	-	++	+++	++	+	-	-	-	+	++	+	+++	++	+	-	-	+	++	+	+	+	+
FLM-2	-	+	++	+++	++	+	-	-	-	+	++	++	+++	++	-	-	-	++	++	-	-	+	+
MA-1	+	+	++	+++	++	++	+	-	-	+	++	++	+++	++	-	-	-	+	++	+	-	+	+
MA-2	+	+	++	+++	++	++	+	-	-	+	++	++	+++	++	-	-	-	+	++	+	-	+	+
JSM1-1	-	+	++	+++	++	+	+	-	-	+	++	++	+++	+++	++	+	+	+	++	+	-	+	+
JSM1-3	-	+	++	+++	++	+	+	-	-	+	++	++	+++	+++	++	+	+	+	++	+	-	+	+
MC5-1	-	+	+++	+++	++	++	+	+	++	++	+++	++	+++	++	+	-	-	++	+	+	-	+	+
MC7-1	-	+	+++	+++	++	++	+	+	++	++	+++	++	+++	++	+	-	-	++	++	+	-	+	+
R1-1	+	++	+++	+++	++	++	+	+	++	+++	+++	++	+++	++	+	-	-	++	+	+	-	+	+

+++, abundant; ++, good; +, fair; w, weak

4. Chemotaxonomic characteristics of actinomycetes strains

The selected strains PNK1-3 and FLM-2 showed the same pattern of chemotaxonomic characteristics which were similar to those of members of the family *Streptomycetaceae* (Tables 12 to 16). Cell wall hydrolysates of them contained glutamic acid, glycine, alanine, and diaminopimelic acid. The isomers of diaminopimelic acid of PNK1-3 contained LL-diaminopimelic acid (LL-DAP), but FLM-2 were LL, and *meso*-DAPs. The acyl types of cell wall muramic acid were N-acetyl type. Characteristic phospholipids were phosphatidylethanolamine, diphosphatidylglycerol, phosphatidylinositol, phosphatidylinositolmannosides, and but. not phosphatidylcholine. This pattern corresponds to phospholipid type II as described by Lechevalier *et al.*, (1977). The cellular fatty acid compositions were shown in Table 14. Their major fatty acids were anteiso-$C_{15:0}$, iso-$C_{15:0}$, $iso_{16:0}$, iso-$C_{17:0}$, and $C_{17:0}$. This pattern corresponds to fatty acid type 3b Kroppenstedt (1985). Mycolic acids were absent. The predominant menaquinones of PNK1-3 were MK-9(H_6), MK-9(H_8), MK-10(H_4) and MK-10(H_6), and small amounts of MK-9(H_4), MK-9(H_2), and MK-10H_8) were also present. Their G+C contents of the DNA of PNK1-3 was 72.9 mol%. On the basis of morphological and chemotaxonomic characteristics and phylogenetica analysis, FLM-2 was classified into the genus *Kitasatospora*.

Seven strains of *Micromonospora* showed the same pattern of chemotaxonomic characteristics which were similar to those of members of the genus *Micromonospora* (Tables 12 to 16). All seven strains had diphosphatidylglycerol, phosphatidylethanolamine and phosphatidylinositol, but not phosphatidylcholine (phospholipids type PII as described by Lechevalier *et al*). Cell wall hydrolysates of them contained glutamic acid, glycine, alanine and *meso*-DAP indicating that these strains have cell wall chemotype II as described by Lechevalier and Lechevalier (1970) and peptidoglycan type Al_γ, as described by Schleifer and Kandler (1972). The acyl type of cell wall muramic acid was glycolyl type. Whole cell sugars were glucose, xylose, arabinose, galactose, mannose and ribose (whole-cell sugar pattern D as described by Lechevalier and Lechevalier, 1970). The fatty acid pattern shown in Table 14 was representative for the *Micromonospora* genus (fatty acid type 3b Kroppenstedt, 1985). Their major fatty acids were iso-$C_{15:0}$, iso-$C_{16:0}$, iso-$C_{17:0}$, anteiso-$C_{15:0}$, $C_{17:0}$, and iso-$C_{17::1}$(ω9c). Mycolic acids could not be found. The predominant menaquinones were MK-10(H_4), MK-10(H_6), MK 10(H_8), MK-9(H_4), and MK-9(H_6), and small amounts of MK-9(H_8), MK-10(H_0), MK-9(H_2), and MK-11(H_4) were also present. Their DNA G+C contents ranged from 71.9 and 72.9 mol%.

Table 12. Diaminopimelic acid types of the actinomycetes strains

Isolate no.	Diaminopimelic acid type		
	meso-DAP	LL-DAP	OH-DAP
PNK1-3	-	+	-
FLM-2	+	+	-
MA-1	+	Trace amount	-
MA-2	+	Trace amount	-
JSM1-1	+	Trace amount	-
JSM1-3	+	Trace amount	-
MC5-1	+	Trace amount	-
MC7-1	+	Trace amount	-
R1-1	+	Trace amount	-

Table 13. Polar lipid composition and glycolic analyses of the actinomycetes strains

Isolate no.	Polar lipid type						Glycolic acid (nM)
	DPG	PIMs	PI	PE	Methyl-PE	OH-PE	
PNK1-3	+	+	+	+	-	-	7.2
FLM-2	+	+	+	+	-	-	8.0
MA-1	+	+	+	+	-	-	119.8
MA-2	+	+	+	+	-	-	76.8
JSM1-1	+	+	+	+	-	-	90.8
JSM1-3	+	+	+	+	-	-	40.5
MC5-1	+	+	+	+	-	-	63.19
MC7-1	+	+	+	+	-	-	111.8
R1-1	+	+	+	+	-	-	76.85

DPG, Diphosphatidylglycerol; PIMs,Phosphatidylinositolmannosides; PI, Phosphatidylinositol

PE, Phosphatidylethanolamine; Methyl-PE, methylphosphatidylethanolamine;

OH-PE, Hydroxyphosphatidylethanolamine

Table 14 Fatty acid compositions of the representative actinomycete strains

Fatty acid	% fatty acid of representative strains								
	PNK1-3	FLM-2	MA-1	MA-2	JSM1-1	JSM 1-3	MC5-1	MC7-1	R1-1
Saturated fatty acid									
$C_{10:0}$	-	-	-	-	-	-	-	-	-
$C_{11:0}$	-	-	-	-	-	-	-	0.1	-
$C_{12:0}$	-	-	-	-	-	-	-	-	-
$C_{13:0}$	-	-	-	-	-	-	-	0.2	-
$C_{14:0}$	-	0.5	-	-	-	-	-	0.9	-
$C_{15:0}$	1.1	2.1	2.2	0.7	0.8	0.3	0.7	0.4	-
$C_{16:0}$	8.7	17.0	0.3	0.2	0.9	0.6	0.5	0.3	0.1
$3OH\text{-}C_{16:0}$	-	-							-
$C_{17:0}$	0.5	-	1.5	0.9	4.9	4.0	3.4	1.3	-
$C_{17:0}$ cyclo	3.2	2.2	-	-	-	-	-	-	-
$3OH\text{-}C_{17:0}$	-	-	0.1	-	-	-	-	-	0.2
$C_{18:0}$	-	-	0.1	0.1	1.4	-	0.8	0.9	-
$C_{19:0}$	-	-	0.1	0.1	0.4	0.3	0.6	0.2	-
Unsaturated fatty acid									
$C_{15:1}(\omega 6c)$	0.3	-	0.5	0.3	0.1	-	-	-	-
$C_{15:1}(\omega 8c)$	-	-	0.1	0.1	0.1	0.1	-	-	-
$2OH\text{-}C_{16:1}$	-	-	-	0.6	-	0.3	3.7	-	3.5
$C_{16:1}(\omega 7c)$	-	7.1	-	-	-	-	-	-	-
$C_{17:1}(\omega 7c)$	-	0.5	-	-	-	-	-	-	-
$C_{17:1}(\omega 8c)$	0.10	4.8	4.6	5.1	12.7	12.6	4.4	2.4	0.6
$C_{17:1}(\omega 9c)$	1.1	0.5	-	4.0	-	-	-	-	-
$C_{18:1}(\omega 7c)$	-	-	-	-	0.1	-	-	-	-
$C_{18:1}(\omega 9c)$	-	-	0.2	0.6	4.5	2.3	1.4	0.7	0.8
$C_{18:3}(\omega 6,9,12c)$	-	-	-	-	-	-	0.2	0.1	2.3

Table 14 Fatty acid compositions of the representative actinomycete strains (continued)

Fatty acid	%fatty acid of representative strains								
	PNK1-3	FLM-2	MA-1	MA-2	JSM1-1	JSM 1-3	MC5-1	MC7-1	R1-1
Branched fatty acids									
i-$C_{11:0}$	-	-	-	0.2	-	-	-	-	-
a-$C_{11:0}$	-	-	-	0.1	-	-	-	-	-
3OH-i-$C_{11:0}$	-	-	-	-	-	-	-	-	-
i-$C_{12:0}$	-	-	0.1	0.2	-	-	-	-	-
i-$C_{13:0}$	0.5	-	0.4	0.6	0.2	-	0.1	0.2	0.1
a-$C_{13:0}$	0.2	-	0.2	0.2	0.1	-	-	-	-
i-$C_{14:0}$	5.4	4.5	1.3	0.5	0.7	0.6	0.3	0.9	0.6
3OH-i-$C_{14:0}$	-	-	0.1	-	-	-	-	-	-
i-$C_{15:0}$	16.7	16.7	41.4	37.5	25.1	20.1	31.3	29.3	23.3
a-$C_{15:0}$	23.1	11.5	12.3	14.7	4.9	5.1	2.6	2.1	0.7
i-$C_{15:1}$	-	-	0.6	1.5	0.3	0.2	0.2	0.2	-
2OH-$C_{16:1}$	-	-	-	-	-	-	3.7	-	3.5
i-$C_{16:0}$	18.7	25.7	8.9	5.0	16.4	21.6	14.6	31.3	40.9
3OH-i-$C_{16:0}$	-	-	0.4	-	-	-	-	-	-
i-$C_{16:1}$	1.2	5.5	1.0	0.8	0.6	0.9	0.4	1.0	2.3
i-$C_{17:0}$	6.1	4.5	4.8	7.0	7.9	5.4	11.3	8.1	6.4
a-$C_{17:0}$	8.2	5.8	6.2	10.7	6.9	7.7	8.3	5.5	1.7
3OH-$C_{17:0}$	-	-	0.1	-	-	-	-	0.2	0.2
a-$C_{17:1}$	-	5.8	0.2	-	-	-	-	-	-
i-$C_{17:1}$ (ω9c)	1.1	4.6	5.1	-	6.4	6.9	5.6	5.6	11.0
a-$C_{17:1}$ (ω9c)	0.6	-	-	0.5	0.5	0.6	0.4	0.4	0.3
i-$C_{18:0}$	0.2	-	-	-	0.3	0.4	0.4	1.4	0.8
i-$C_{18:1}$	-	-	-	-	-	-	0.2	0.2	0.2

Table 14 Fatty acid compositions of the representative actinomycete strains (continued)

Fatty acid	%fatty acid of representative strains								
	PNK1-3	FLM-2	MA-1	MA-2	JSM1-1	JSM 1-3	MC5-1	MC7-1	R1-1
10-Methyl fatty acids									
$C_{16:0}$	-	-	2.2	-	-	-	-	-	-
$C_{17:0}$	-	-	8.7	5.7	1.2	5.7	5.8	6.1	4.5
$C_{18:0}$ TBSA	-	-	0.6	0.7	0.4	0.9	1.6	1.1	1.0
Summed feature 3[b]	2.9	1.5	0.3	0.5	0.9	0.3	0.1	0.1	-
Summed feature 6[b]	-	-	-	0.3	0.4	0.6	0.8	0.3	0.7

[a] Values are percentages of total cellular fatty acids.

[b] Summed features represent groups of one or two fatty acids which could not be separated by GLC with the MIDI system. Summed feature 3 contained one or more of the following fatty acids : 2-OH-i-C_{15} : 0 and/or $C_{16:1}$ (ω7c). Summed feature 6 contained one or more of the following fatty acids : $C_{19:1}$(ω11C) /C19 : 1 (ω9c).

Table 15 Menaquinone types of the representative strains

Isolate no.	G+C (%mol)	% of Menaquinone type								
		MK-9(H_2)	MK-9(H_4)	MK-9(H_6)	MK-9(H_8)	MK-10(H_0)	MK-10(H_2)	MK-10(H_4)	MK-10(H_6)	MK-10(H_8)
PNK1-3	72.5	Trace	Trace	41.0	29.0	-	-	6.7	2.7	trace
MA-1	72.5	Trace	8.5	5.9	Trace	Trace	1.3	48.1	25.7	4.3
MA-2	72.1	Trace	7.1	4.5	Trace	Trace	Trace	53.0	25.8	3.6
JSM1-1	72.0	Trace	6.0	2.1	-	Trace	2.8	52.0	22.2	3.7
JSM1-3	71.9	Trace	5.9	2.3	-	Trace	2.5	55.0	18.3	6.1
MC5-1	72.8	1.2	Trace	9.5	19.0	Trace	1.2	Trace	15.5	51.1
MC7-1	72.7	-	Trace	9.2	12.2	Trace	Trace	Trace	22.2	45.7
R1-1	72.9	-	2.8	17.7	9.2	Trace	Trace	3.1	30.6	20.0

Table 16 Whole cell sugar of the representative strains

Isolate no.	Whole cell sugar type						
	Rhamnose	Ribose	Mannose	Arabinose	Galactose	Xylose	Glucose
MA-1	+	+	+	+	+	+	+
MA-2	+	+	+	+	+	+	+
JSM1-1	Trace amount	+	+	+	+	+	+
JSM1-3	Trace amount	+	+	+	+	+	+
MC5-1	-	+	+	+	+	+	+
MC7-1	-	+	+	+	+	+	+
R1-1	-	+	+	+	+	+	+

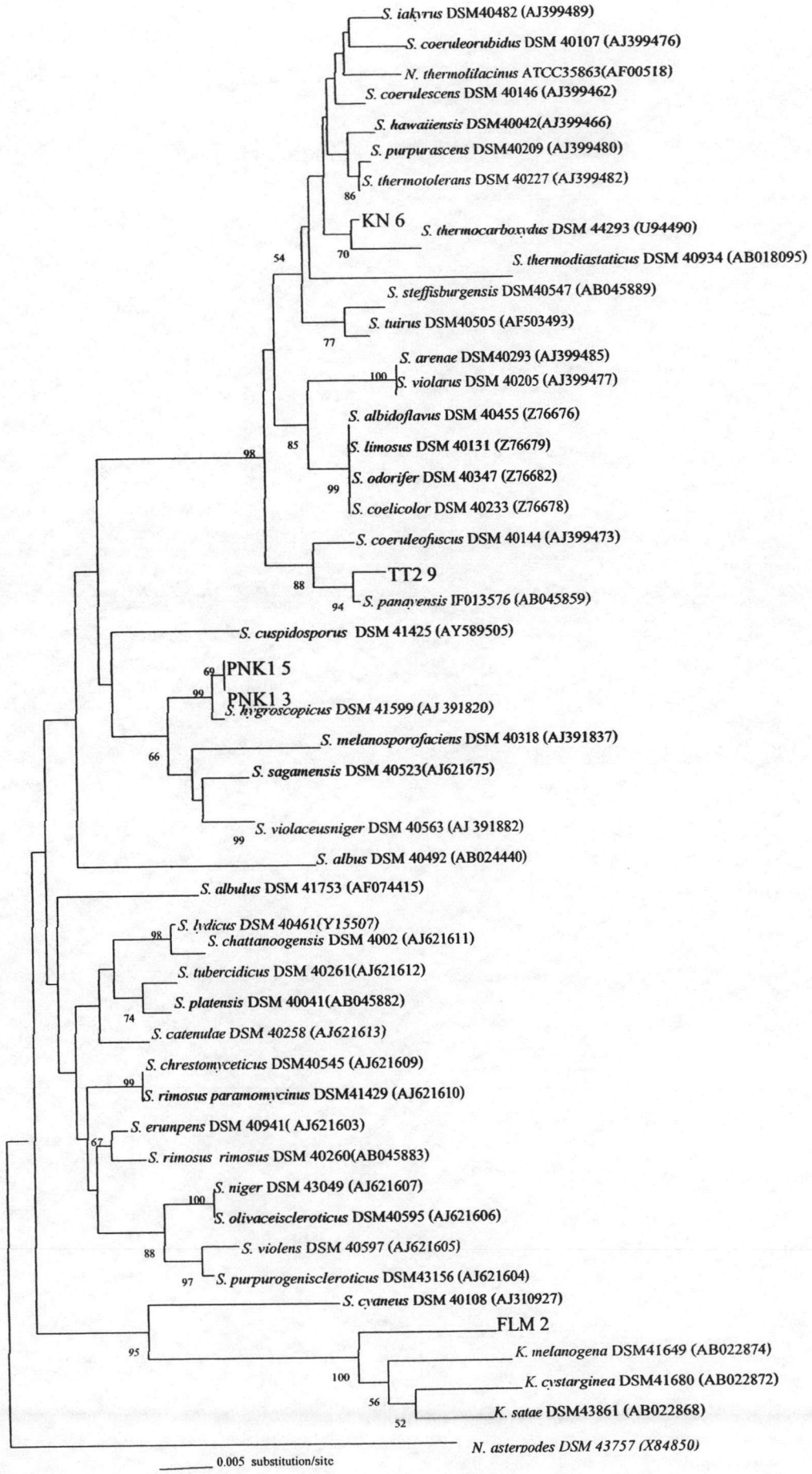

Figure 6 Unroot neighbor-joining tree base on nearly complete 16S rDNA sequences, showing the position of the PNK1-3, PNK1-5, KN-6, TT2-9 and FLM-2 strains

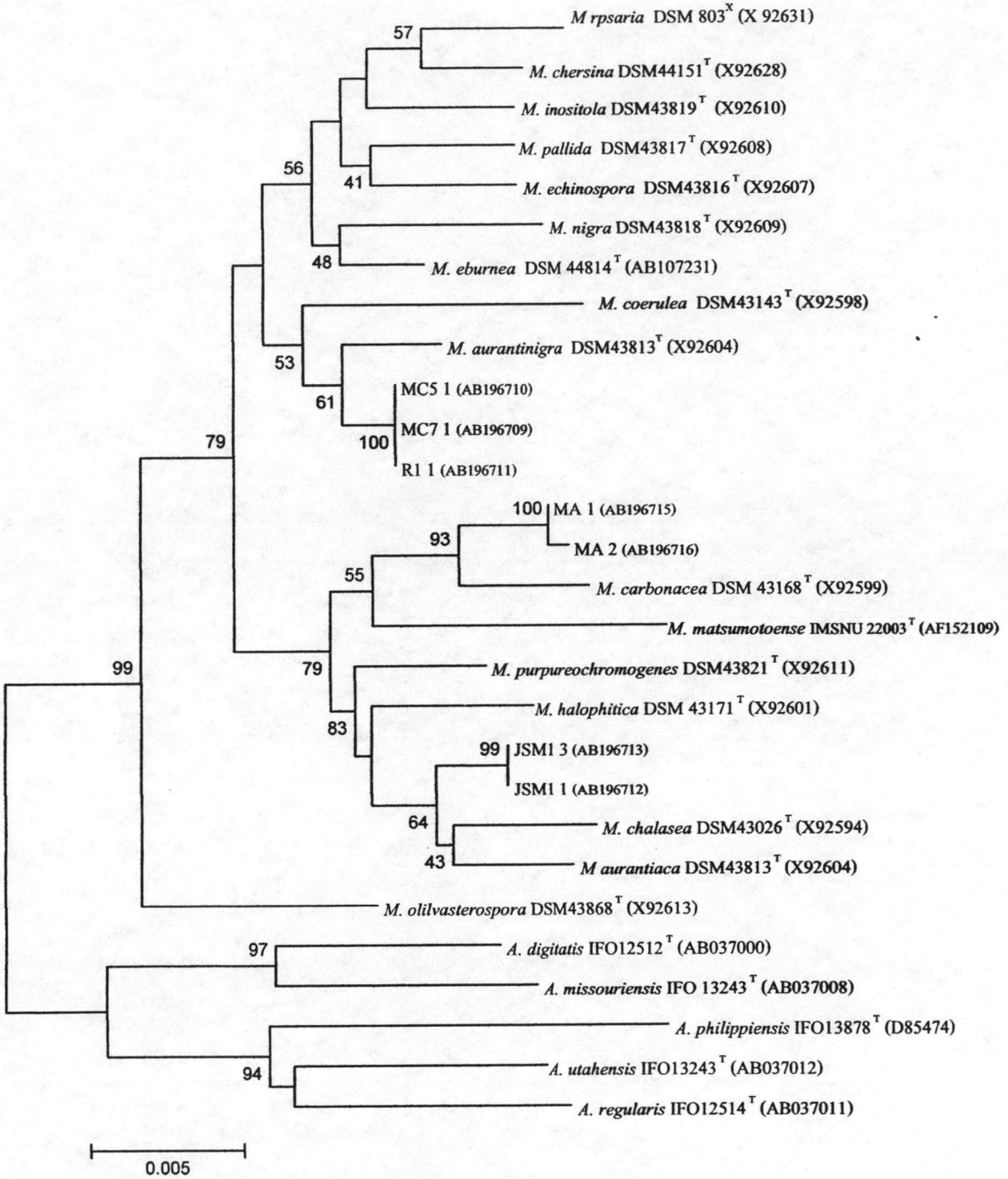

Figure 7 Unroot neighbor-joining tree base on nearly complete 16S rDNA sequences, showing the position of the representative *Micromonospora* strains

5. 16S rDNA Amplification and nucleotide sequence analysis

5.1 16S rDNA sequencing

The PCR products of all of the strains were determined for their 16S rDNA nucleotide sequences. Their nucleotide sequences were illustrated in Appendix VI. The 16S rDNA sequence alignment results between the representative strains and some of validly described *Streptomyces*, *Kitasatospora*, and *Micromonospora* species are shown in Figures 8 and 9.

5.2 16S rDNA sequence and phylogenetic tree analysis

The almost complete 16S rDNA sequence consisting of 1,380-1,510 nucleotides were determined for some type strains of *Streotomyces, Kitasatospora* and *Micromonospora.* All representative strains of *Micromonospora* were used for phylogenetic analysis, similarity percentage calculation, and complared with 16S rDNA database sequences of members of the family *Streptomycetaceae and Micromonosporaceae.* The phylogenetic tree was constructed from evolutionary distances by using neighbor joining method in the MEGA software program version 2.1

Phylogenetic analysis of the strains which carried out with available, almost complete 16S rDNA nucleotide (1,338 nt fragment) obtained from strains PNK1-3, PNK1-5, TT2-9, KN-6 and FLM-2 some of the type strains of validly described *Strptomyces* species, *Kitasotospora* species, and the 16S rDNA sequence of *Nocardia asterioides* as an outgroup (Figure 6). The strains of PNK1-3 and PNK1-5 were 99.9% related to each other and shared 16S rDNA nucleotide similarities within 99.9% with *S. hygroscopicus* DSM 41599 which correspond to 2 nucleotide differences. These organisms were most closely associated in the neighbor-joining analysis by a highly bootstrap value and shared the highest similarity percentage. Hence, this strain should be identified as *S. hygroscopicus.* The strains TT2-9 and KN-6 showed 99.6% and 99.5% similarities with *S. panayensis* IFO 13576 and *S. thermocarboxydus* DSM 44293, respectively. FLM-2 was most closely related the type strain of *K. melanogena* DSM41649, and which was supported by a highly bootstrap value of 100%; the two organisms shared 16S rDNA nucleotide similarity value of 97.1%. However the DNA-DNA relatedness studies should resolve the fine taxonomic relationship to separate it as a new species.

Phylogenetic analysis of *Micromonospora*, the almost complete 16S rDNA sequences of the tested organisms with the corresponding sequences of all of the type strains of validly described *Micromonospora* species, selected sequences of *Actinoplanes* (as an out group) species

showed that the strains of *Micromonospora* groups I, II, and III could be distinguished both for one another (Figure 7). It is evident from figure 7 that the groups II strains form distinct phyletic lines in the 16S *Micromonospora* rDNA tree, and the groups I, II and III strains form subclade with *M. carbonaceae* DSM 43168 ^{T}, *M. chalchea* DSM43026^{T} and *M. aurantinigra* DSM 43813^{T},respectively.

The almost complete 16S rDNA sequences data (1437) of two strains of *Micromonospora* group I (MA-1 and MA-2^{T}) showed 16S rDNA nucleotide sequences and were most closely related to each other (99.7% sequence similarity) and clustered 99.0% sequence similarity with *M. carbonaceae* DSM 43168 ^{T}. Strain MA-2^{T} showed a different physiological and biochemical pattern compared to the phylogenetically closest species, *M. carbonaceae* DSM 43168^{T}. In particular, the utilization of D-mannitol, D-raffinose, D-rhamnose, and D-ribose and the growth at temperature 45 ^{o}C effectively discriminates strain MA-2^{T} from *M. carbonaceae* DSM 43168^{T} (Table 21). The level of DNA-DNA similarity between strains MA-2^{T} and *M. carbonaceae* DSM 43168^{T} from 30.1%. These representative strains were unidentified.

The representative strains of *Micromonospora* group II JSM1-1^{T}and JSM1-3 was most closely related to the type strains *M. chalcea* DSM 43026^{T} and *M. aurantiaca* DSM 43813^{T}. They showed a 16S rDNA gene 99.0% sequence similarity to *M. chalcea* DSM 43026^{T} and 98.9% sequence similarity to *M. aurantiaca* DSM 43813^{T}. DNA-DNA relatedness studies were not carried out between these isolates and type strain of *M. chalcea* DSM 43026^{T}, since the isolates showed significant difference in physiological and biochemical properties from those of the phylogenetically closest species i.e. *M. chalcea* DSM43026^{T}. In particular, the result of the growth at temperature 45 ^{o}C, the maximum NaCl concentration for growth, decomposition of tyrosine and utilization of D-manitol, D-ribose, glycerol and L-arabinose effectively discriminates strain JSM1-1^{T} from *M. chalcea* DSM 43026^{T}.

The analysis of almost complete 16S rDNA sequence (1436) of *Micromonospora* group III (MC5-1^{T}, MC7-1 and R1-1) were compared with those selected members *Micromonospora*. Strains MC5-1^{T}, MC7-1 and R1-1 were 99.8% related to each other and cluster (99.3% sequence similarity) with *M. aurantinigra* DSM43813^{T} and which supported by a bootstrap value of 100% in the neighbor-joining. Strain MC5-1^{T} showed difference in physiological and biochemical properties which were distinguished in the utilization of D-manitol, D-ribose and D-raffinose. In particular, the result of maximum NaCl tolerance test was 3% and growth tolerance at pH 4 were

effectively discriminated from *M. aurantinigra* DSM43813^T (Table 21). In additional, the level of DNA-DNA similarity among strains MC5-1^T, MC7-1 and R1-1 ranged from 79.5 to 88.5% while the level of DNA-DNA similarity between three isolates and *M. aurantinigra* DSM43813^T was 43 %. Hence, these representative strains were unidentified.

6. Comparison of DNA-DNA similarity of strains

The strains of *Micromonospora* group I showed DNA-DNA similarity values of 35.8% similar to *M. carbonaceae* DSM 43168^T, and group III showed DNA-DNA similarity values 40.3% to *M. auratinigra* DSM43813^T, respectively (Tables 17 and 18). The values are well lower than the 70% recommended by Wayne *et al.*, (1987), so, they could not be classified as any known species of the genus *Micromonospora*. Result of DNA-DNA similarity of group II (JSM1-1^T and JSM1-3) showed that values of clearly above 70% (95-97%) were obtained the same species (Table 19).

Table 17 DNA-DNA similarity among the *Micromonospora* group I and group II

Isolate no.	Percentage DNA complementary with labeled DNA		
	MA-1	MA-2^T	DSM 43168^T
MA-1	100	80.3	35.8
MA-2^T	84.8	100	29.1
M. carbonacea DSM 43168^T	39.2	30.1	100
	JSM1-1	JSM1-3	
JSM1-1	100	95	
JSM1-3	97	100	

Table 18 DNA-DNA similarity among the *Micromonospora* group III

Isolate no.	Percentage DNA complementary with labeled DNA			
	MC5-1^T	MC7-1	R1-1	DSM43813^T
MC5-1^T	100	88.5	79.5	37.9
MC7-1	85.2	100	81.9	33.5
R1-1	79.7	81.5	100	40.3
M.auratinigra DSM43813^T	43	38.3	43.4	100

7. Characteristics of one known *Streptomyces* species and three novel *Micromonospora* species (Tables 11-21)

7.1 Characteristics of *Streptomyces* PNK1-3

PNK1-3 is gram-positive, mesophilic aerobic bacteria possessing non-motile spores that forms well developed an extensively branched substrate and aerial mycelium at maturity form long chains spiral spores. Vegetative mycelium developed on most media when sporulation occured, the surface of the colony turned from white color to black at 30 °C for 21 days. PNK1-3 could utilize D-galactose, D-glucose, D-fructose, D-mannitol, D-melibiose, D-rafinose, D-xylose, but weakly utilized glycerol and salicin sole carbon sources for energy. Hydrolysis of starch, gelatin liquefaction, milk peptonization were positive. PNK1-3 could decompose L-tyrosine, but not adenine, hypoxanthine, and xanthine. Well growth was observed between 25 and 30 °C. No growth occurred above 40 °C. The range of NaCl concentration for growth was 3%. Cell wall peptidoglycan contains glutamic acid, glycine, alanine, and L-diaminopimelic acid. The acyl type of the cell wall is N-acetyl. The phospholipid profile (type II) contains phosphatidylinositolmannosides, diphosphatidylglycerol, phosphatidylinositol and phosphatidylethanolamine, but not phosphatidylcholine. The major cellular fatty acids are iso-$C_{15:0}$, anteiso-$C_{15:0}$, and iso-$C_{16:0}$, and a small amounts of iso-$C_{17:0}$, and anteiso-$C_{17:0}$ are also present. Mycolic acids are absent. The predominant menaquinones are MK-10(H_4), and MK-10 (H_6). The G+C content of the DNA is 72.9 mol%. Habitat is soil.

7.2 Characteristics of *Kitasatospora* FLM-2

FLM-2 comprises a group of filamentous and aerobic gram-positive that form an extensively branched substrate and aerial mycelium bearing long spore chains of more than 20 spores. Vegetative mycelium developed on most media when sporulation occured, the surface of the colony turned from white pale gray color to dark gray at 30 °C for 21 days. FLM-2 could utilize D-galactose, D-glucose, Lactose, D-melibiose, D-xylose, L-arabinose but weakly utilized salicin, D-ribose, D-fructose, as sole carbon sources for energy. Hydrolysis of starch, milk peptonization are positive. Adenine, hypoxanthine, xanthine, L-tyrosine and gelatin were not decomposed. Well growth was observed between 25 and 30 °C. No growth occurred above 40 °C. The range of NaCl concentration for growth was 3%. Cell wall peptidoglycan contains glutamic acid, glycine, alanine, L and *meso*-diaminopimelic acid. The acyl type of the cell wall is N-acetyl. The phospholipid profile contains phosphatidylinositolmannosides, diphosphatidylglycerol,

phosphatidylinositol and phosphatidylethanolamine, but not phosphatidylcholine (type II). The major cellular fatty acids are iso-$C_{15:0}$, anteiso-$C_{15:0}$, and iso-$C_{16:0}$, and small amounts of iso-$C_{17:0}$, and anteiso-$C_{17:0}$ are also present. Mycolic acids are absent. The G+C content of the DNA is 73.1 mol%. Habitat is soil.

7.3 Characteristics of three novel *Micromonospora*

MA-2^T, JSM1-1^T and MC5-1^T are gram-positive, mesophilic aerobic bacteria; non-motile actinomycete that forms well developed an extensively branched substrate mycelium. No aerial mycelium produced. Vegetative mycelium developed on most media when sporulation occured, the surface of the colony turn from orange color to black at 30 °C for 21 days. Single spores are formed on the substrate hyphae. Cell wall peptidoglycan contains glutamic acid, glycine, alanine, and *meso*-diaminopimelic acid. The acyl type of the cell wall is N-glycolyl. The characteristic whole cell sugars are xylose and arabinose. The phospholipid profile contains diphosphatidylglycerol, phosphatidylinostiolmannosides, phosphatidylinositol and phosphatidylethanolamine, but not phosphatidylcholine. The major cellular fatty acids are iso-$C_{15:0}$, anteiso-$C_{15:0}$, and iso-$C_{16:0}$, and small amounts of iso-$C_{17:0}$, and anteiso-$C_{17:0}$ are also present. Mycolic acids are absent.

Micromonospora Group I

MA-1 and MA-2 could utilize D-galactose, D-glucose, D-fructose, D-mannitol, D-melibiose, D-rafinose, salicin, D-xylose, L-arabinose, but weakly utilized D-ribose, L-rhamnose and lactose as sole carbon sources for energy. Hydrolysis of starch, gelatin liquefaction, milk peptonization were positive. *Micromonospora* group I could decompose L-tyrosine, but not adenine, hypoxanthine, and xanthine. Well growth was observed between 25 and 30 °C. No growth occurred above 45 °C. The range of NaCl concentration for growth was 3%. The predominant menaquinones are MK-10(H_4) and MK-10 (H_6). The G+C content of the DNA is 72.1 mol%. Habitat is soil. *Micromonospora krabiensis* sp. nov. is proposed for Group I (2 strains).

Micromonospora Group II

JSM1-1 and JSM1-3 could utilize D-galactose, D-glucose, D-fructose, D-melibiose, D-raffinose, D-xylose, L-arabinose, but not lactose, L-rhamnose and salicin as sole carbon sources for energy. Hydrolysis of starch, gelatin liquefaction, and milk peptonzation were positive. They could decompose L-tyrosine, but not adenine, hypoxanthine, and xanthine. Well growth was

observed between 25 and 30 °C. No growth occurred above 45 °C. The range of NaCl concentration for growth was 7 %. The predominant menaquinones are MK-10(H_4), MK-10(H_6), and MK-9 (H_8). The G+C content of the DNA is 72.0 mol%. Habitat is soil. *Micromonospora marinus* sp. nov. is proposed for group II (2 strains).

***Micromonospora* Group III**

MC5-1, MC7-1 and R1-1 could utilize D-galactose, D-glucose, D-fructose, D-melibiose, glycerol, salicin, D-xylose, L-arabinose, lactose, but not D-ribose, L-rhamnose and D-mannitol as sole carbon sources for energy. Hydrolysis of starch, gelatin liquefaction, and milk peptonization were positive. Decompose L-tyrosine, but not adenine, hypoxanthine, and xanthine. Well growth was observed between 25 and 30 °C. No growth occurred above 45 °C. The range of NaCl concentration for growth was 4%. The predominant menaquinones are MK-10(H_8), and MK-9 (H_8), and MK-10(H_6). The G+C content of the DNA is 72.8 mol%. Habitat is soil. *Micromonospora chaiyaphumensis* sp. nov. is proposed for Group III (3 strains).

Table 19 Differential characteristics of representative strains and all type strains *Micromonospora*

Characteristic	PNK1-3	FLM-2	MA-2	JSM1-1	MC5-1	1	2	3	4	5	6	7	8	9	10	11	12	13	14	15	17	18
Nitrate reduction	+	-	-	-	-	-	-	-	w	-	-	-	-	+	-	w	-	-	-	-	+	-
Peptonization of milk	+	+	+	+	+	+	+	-	w	+	+	+	+	+	+	-	-	+	-	w	+	+
Starch hydrolysis	+	+	+	+	+	+	+	w	-	+	+	+	w	+	+	+	+	+	+	+	+	+
Gelatin liguefaction	+	-	+	+	+	+	+	+	-	+	+	+	+	+	+	+	+	+	-	+	+	+
Decomposition of Tyrosine	+	-	+	+	+	-	-	-	-	-	-	-	-	+	-	-	-	-	-	-	-	+
Growth that at																						
40 °C	+	+	+	+	+	+	+	+	+	+	+	+	+	+	+	+	+	+	+	+	+	+
45 °C	-	-	+	+	+	-	+	-	-	+	+	-	+	+	-	+	+	-	-	+	+	-
Max NaCl tolerance (%)	4	3	4	7	4	1.5	5	2	1.5	3	3	3	2	4	3.5	4	3.5	3.5	4	2.5	4	3
Utilizattion of :																						
D-Manitol	+	-	+	w	-	-	-	-	-	-	-	-	w	-	-	-	-	-	-	-	w	-
D-Ribose	+	w	w	+	-	w	-	-	-	+	w	w	+	-	-	-	w	-	-	+	w	-
L-Rhamnose	+	+	w	-	-	-	-	-	-	-	+	-	+	-	-	-	-	-	-	+	+	-
D-Melibiose	+	+	+	+	+	+	+	+	+	w	-	+	+	+	+	+	+	+	+	+	+	+
D-Raffinose	+	-	+	+	+	+	+	w	+	-	-	+	w	w	+	+	+	-	+	+	+	w
Glycerol	w	-	-	w	w	-	-	-	-	-	w	-	-	-	+	-	+	w	+	-	w	-
Salicin	w	w	+	-	+	w	-	-	w	-	w	w	w	-	+	+	+	+	+	+	+	+
Lactose	+	+	w	-	+	+	+	w	+	w	+	+	+	+	+	+	+	+	+	+	+	+
D-Galactose	+	+	+	+	+	+	+	+	+	+	+	+	+	+	+	w	+	+	W	+	+	+
L-Arabinose	-	+	+	+	+	+	w	w	-	-	+	+	+	+	-	-	+	-	-	+	-	+

1, *M. coerulea* JCM 3175^T; 2, *M. chalcea* JCM 3031^T; 3, *M. inositola* JCM6239^T; 4, *M. purpureochromogenes* JCM 3156^T; 5, *M. olivasterospora* JCM 7.48^T; 6, *M. echinospora* JCM 3073^T; 7, *M. matstattmotoense* JCM 9401^T; 8, *M. rosaria* JCM 3159^T; 9, *M. aurantiaca* JCM 1084^T; 10, *M. nigra* JCM 8973^T; 11, *M. halophytica* JCM 3125^T; 12, *M. chersina* JCM 9459^T, 13, *M. carbonacea* JCM 3139^T; 14, *M. pallida* JCM 3133^T; 15, *M. auratinigra*JCM 12357^T; 16, *M. eburnea* JCM 12345^T; 17, *M. endolithica* JCM 12677^T; +, positive, -, negative, w, weakly positive.

8. Structure elucidation of compounds from PNK1-3 and *M. kaoliang*

8.1 Structure elucidation of PNK01

Compound PNK01 was obtained as a yellow amorphous powder showing optical rotation $[\alpha]^{25}_{D}$ +48.2° (c.050, $CHCl_3$). The IR absorption spectrum (Figure23) displayed characteristic bands of OH stretching at 3441 cm^{-1}, C=O stretching at ν 1735 cm^{-1}, and C=O stretching, amide I band at ν 1,654 cm^{-1}. The UV spectrum in $CHCl_3$ of compound PNK01 exhibited λ_{max} at 216, 262 and 307 nm (Figure22). The ESI mass spectrum of this compound exhibited [*m/z* 583.20 $(M + Na)^+$ (Figure 24)].

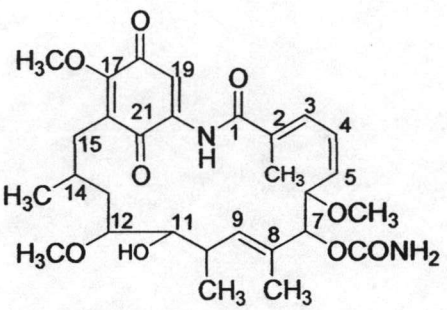

The ^{1}H-NMR spectral data ($CDCl_3$) (Figure 25) of PNK01 showed four methyl groups at δ_H 0.76 (3H), 0.97 (3H), 1.61 (3H) and 1.92 (3H), three methoxy protons at δ_H 3.22 (3H, *s*), 3.32 (3H, *s*), and 3.95 (3H, *s*) two methylene protons at δ_H 1.45 (2H, m), and 2.49 (2H, m); four olefinic protons at δ_H 6.95 (1H, *d*, *J* = 12 Hz), 6.57 (1H, *t*, *J* = 12, 11 Hz), 5.83 (1H, *t*, *J* = 10, 10 Hz), 5.51 (1H, *t*, *J* = 10, 10 Hz), four oxygenated methines at δ_H 4.34 (1H, *d*, *J* = 10 Hz), 4.88 (1H, *brs*), 3.22 (1H, *m*), 3.08 (1H, *m*), eleven methine protons at δ_H 1.92 (1H, brs), 3.07 (1H, m), 3.22 (1H, m), 3.62 (1H, m), 4.34 (1H, d, *J* = 10), 4.88 (1H, brs), 5.51 (1H, d, *J* = 10), 5.83 (1H, t, *J* = 10, 10), 6.57 (1H, t, *J* = 12, 11), and 6.95 (H-3), and two exchange protons at δ_H 6.45 (OCONH2) and 9.16 (-NH) ppm.

The ^{13}C-NMR spectrum (Figure 28) exhibited 29 signals which were classified by the DEPT 135 and HMQC spectra as four methyl carbons at δc 12.2 (2-Me), 12.5 (8-Me), 13.0 (14-Me) and 23.3 (10-Me), three methoxy carbons at δc 56.0 (6-OMe), 56.5 (12-OMe), 61.1 (17-OMe), two methylene carbons at δc 30.9 (C-13), 31.7(C-15), eleven methine carbon signals at δc 26.6 (C-14), 32.1 (C-10), 71.9 (C-11), 80.2 (C-12), 80.63 (C-7), 110.8 (C-19), 125.81 (C-4), 128.2 (C-3), 131.9 (C-9), and 138.0 (C-5) ppm; and nine quarternay carbon signals at δc 128.2 (C-16), 132.7 (C-8), 133.1 (C-2), 139.7 (C-20), 154.9 (7-OCONH2), 156.4 (C-17), 169.2 (C-1),

183.2 (C-21), and 183.7 (C-18). Analysis of the ^{13}C-NMR spectrum indicated the presence of the two quinone carbonyl carbons at 183.2 and 183.7 ppm.

The ^{1}H-^{1}H COSY spectrum (Figure 31) revealed the connectivity in $CDCl_3$ from H-3 through H-7; H-9 through H-13; and 14-Me through H-15. The HMBC spectrum showed the following long-range corrleations; NH (δ_H 9.16) to amide carbonyl carbon C-1 (δc 169.2) and quinone carbonyl carbon C-21 (δc 183.2); 2-Me (δ_H 1.92) to C-1 (δc 169.2), C-2 (δc 133.1), and C-3 (δc 128.2); 8-Me (δ_H 1.61) to C-7 (δc 80.6), and C-8 (δc 132.7); 6-OMe (δ_H 3.22) to C-6 (δc 81.7); 12-OMe (δ_H 3.32) to C-12 (δc 80.2); 17-OMe (δ_H 3.95) to C-17 (156.4), and quinone carbonyl carbon C-18 (δc 183.2); and H-19 (δ_H 7.03) to C-17 (δc 156.4), C-20 (δc 139.7), and C-21 (δc 183.2).

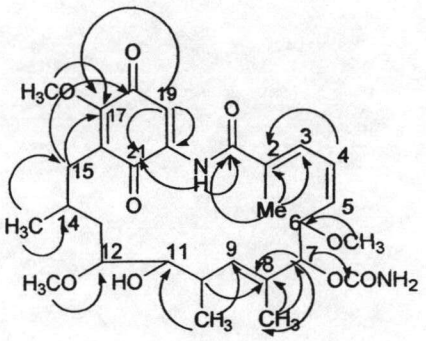

The geometrics of double bonds at C-2 = C-3, C-4 = C-5, and C-8 = C-9 were determined by NOESY experiment. The present corrleations of 2-Me to H-4, H-4 to H-5, H-3 to H-6 and H-7, and H-9 to H-7 and the absent corrleation of H-3 to 2-Me and H-9 to 8-Me suggested that geometrics of double bonds at C-2 = C-3 and C-8 = C-9 are *E* and C-4 = C-5 is *Z*.

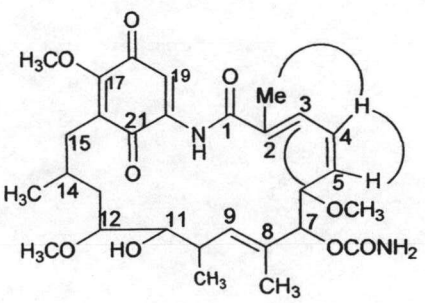

Table 20 Comparison of ^{1}H and ^{13}C NMR spectral data of compound PNK01 with that of geldanamycin (Omura *et al.*, 1979) in DMSO-*d*6.

C	PNK01		Geldanamycin	
	δc, mult.[a]	δ_H, mult., J in Hz	δc, mult.[a]	δ_H, mult
1	169.2, *s*	-	169.1 *s*	-
2	133.1, *s*	-	133.2, *s*	-
2-Me	12.2, *q*	1.92 , s	12.2, *q*	1.91 , s
3	128.2, *d*	6.95, *d*, (12)	128.42, *d*	6.95, *d*
4	125.8, *d*	6.57, *t* (12,11)	125.7, *d*	6.56, *t*
5	138.0, *d*	5.83, NH_2, brs	137.8, *d*	5.80, *t*
6	81.7, *d*	4.34, d. (10)	81.6, *d*	4.34, *d.*
6-OMe	56.0, q	3.22, *s*	56.0, q	3.22, *s*
7	80.6, *d*	4.88, brs	80.6, *d*	4.86, brs
7-$OCONH_2$	154.9, *s*	6.45,brs	156.0, *s*	6.45,brs
8	132.7, *s*	-	132.6, *s*	-
8-Me	12.5, *q*	1.61, *s*	12.5, *q*	1.61, *s*
9	131.9, *d*	5.51, *d*, (10)	131.9, *d*	5.51, *d*
10	32.1, *d*	3.62, m	32.1, *d*	3.61, m
10-Me	23.3, *q*	0.97, d, (7)	23.3, *q*	0.97, d
11	71.9, *d*	3.22. m	71.9, *d*	3.29, *s*
12	80.2, *d*	3.08, m	80.2, *d*	3.07, m
12-OMe	56.5, *q*	3.32, *s*	56.5, *q*	3.23, *s*
13	30.9,*t*	1.45, *m*	31.0, *t*	1.45, *m*
14	26.6, *d*	1.92, *brs*	26.6, *d*	1.91, *brs*
14-Me	13., *q*	0.76, *d*, (6)	13.0, *q*	0.76, *d*
15	31.7, t	2.49, m	31.7, t	2.42, m
16	128.5, s	-	128.1, s	-
17	156.4, s	-	156.4, s	-
17-OMe	61.1, *q*	3.95, *s*	61.0, *q*	3.93, *s*
18	183.8, *s*	-	183.6, *s*	-
19	110.8, *d*	7.03, s	110.9, *d*	7.02, s
20	139.7*s*	-	139.6, *s*	-
21	183.2, *s*	-	183.1, *s*	-
-NH	-	9.16, NH, brs	-	9.14, NH, brs

8.2 Structure Elucidation of Compound Ang01

A compound Ang01 was obtained as yellow viscous liquid. Ang01 possessed a molecular formula $C_{13}H_{18}O_5$, as revealed by the ESITOF mass spectrum, showing a prominent peak at [*m/z* 277.1041 $(M + Na)^+$calculated for 277.1052 (Figure 37)]. The IR spectrum displayed OH stretching at ν 3350 cm^{-1}, CH stretching of alkane at ν 2932 cm^{-1}, C=O stretching at ν 1650 cm^{-1}, CH deformation of CH_2 and CH_3 ν 1409 cm^{-1}, and C-O stretching ν 1193 cm^{-1} (Figure 36). The UV absorption showed λ_{max} at 244 and 346 nm (Figure 35).

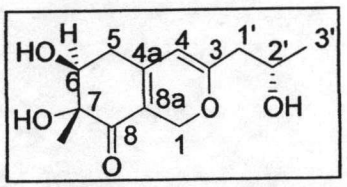

The ^1H NMR spectral data ($CDCl_3$) (Figure 38) (Table 21) of compound Ang01 prominently showed signals of two methyls (as a singlet and a doublet) at δ_H 1.25 (3H, *s*) and 1.24 (3H, *d*, *J* = 6.5), two non equivalent methylene groups at δ_H 2.43 (1H, *ddd*, *J* = 15.1, 10.6, 1.5 Hz), δ_H 2.61 (1H, *dd*, *J* = 15.2, 5.5 Hz), δ_H 4.83 (1H, *dt*, *J* = 12.7, 1.3 Hz), and δ_H 4.93 (1H, *dd*, *J* = 12.6, 1.7 Hz), doublet signal of methylene protons at δ_H 2.34 (1H, *d*, *J* = 6.2 Hz), a singlet olefinic proton (at δ_H 5.28 Hz), and two oxygenated methines at δ_H 4.00 (1H, *dd*, *J* =10.4, 5.7 Hz), and δ_H 4.08 (1H, *m*).

Analyses of ^{13}C NMR spectrum of compound Ang01 revealed the presence of 13 signals, and the DEPT 135 (Figure 40) spectral data revealed three methine carbons δc 66.1 (C-2′) , δc 72.7 (C-6), and δc 103.5 (C-4); three methylene carbons δc 33.9 (C-5), δc 43.8 (C-1′), and δc 64.6 (C-1); two methyl δc 18.3 (C-3′), and δc 23.5 (7-Me); and five quaternary carbons δc 77.6 (C-7), δc 112.9 (C-8a), δc 150.2 (C-4a), δc 165.7 (C-3), δc 197.6 (C-8). The HMQC spectral data of Ang01 (Figure 41) assisted in the assignment of protons attached to their corresponding carbons. Attachment of the unsaturated sp^2 C-3 to an oxygen atom in Ang01 was evident from a downfield shift of its ^{13}C resonance (at δc 165.7). The IR absorption at 1650 cm^{-1}, together with ^{13}C resonance at δc 197.6, confirmed the presence of a conjugated ketone carbonyl in Ang01.

The ^1H–^1H COSY spectrum (Figure 42) of compound Ang01 established the connectivity from H-1′ (δ_H 2.34) through H-3′ (δ_H 1.24) and the coupling between H-6 (δ_H 4.00) and H-5 (δ_H 2.43 and 2.61), and also demonstrated the allylic coupling between H-1′ (δ_H 2.34) and H-4 (δ_H 5.28).

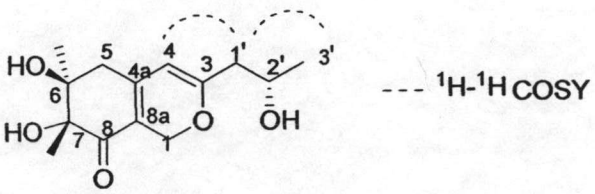

The HMBC spectrum of Ang01 (Figure 46) showed correlations from H-1 (δ_H 4.83 and 4.93) to C-3 (δc 165.7), C-4a (δc 150.2), and C-8a (δc 112.9); H-4 (δ_H 5.28) to C-3, C-5 (δc 33.9), and C-8a; H-5 (δ_H 2.43 and 2.61) to C-4a and C-8a; H-1′ (δ_H 2.34) to C-3 and C-4 (δc 103.5); 7-Me protons (δ_H 1.25) to C-6 (δc 72.7), C-7 (δc 77.6), and C-8 (δc 197.6). On the basis of these spectral data, the structure of Ang01 was therefore identified as 6,7-dihydroxy-3-(2-hydroxy-propyl)-7-methyl-1,5,6,7-tetrahydro-isochromen-8-one. The coupling constants between H-6 and the two adjacent methylene protons of (H-5ax and H-5eq) 10.4 and 5.7 Hz indicated an axial orientation of this proton. The absence of a cross peak between H-6 and 7-Me protons in the NOESY spectrum of Ang01 implied an antirelationship between H-6 and 7-Me.

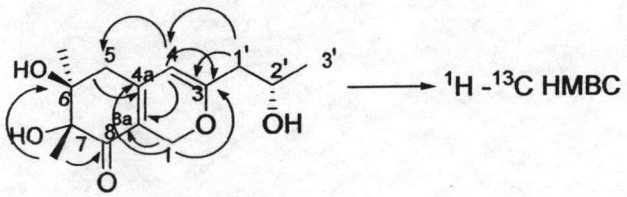

The absolute configuration of Ang01 was addressed by the use of Mosher ester (Dale and Mosher, 1973; Sullivan *et al.*, 1973). However, we found that (*R*) and (*S*)-methoxy trifluoromethylphenyl acetate (MTPA) esters (compounds Ang01a and Ang01b respectively), of Ang01 were not stable and easily degraded to unidentified products during purification of the reaction mixtures. We therefore employed a convenient procedure for the Mosher ester formation, which was carried out in an NMR tube as recently reported by Kinghorn and his colleagues (Su *et al.*, 2002). The Δδ values [δ (-)-δ (+)] are shown in Figure.47, indicating that the absolute configurations at C-2′ and C-6 are *S*. It should be noted that one of the H-5 methylene protons (-0.064 and +0.036) possessed a positive Δδ value (+0.036), and this may raise an uncertainty concerning the absolute stereochemistry of H-6. However, considering the similarity of positive optical rotations for both Ang01 and monascin (Ang03).

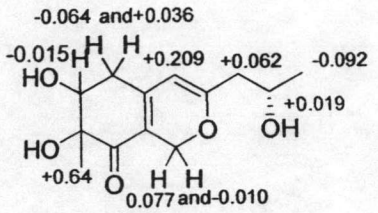

Figure47 $\Delta\delta$ values [$\delta_{(-)}$-$\delta_{(+)}$] for the MTPA ester (Ang01a and Ang01b) of Ang01

Table 21 The ^{1}H (400 MHz) and ^{13}C NMR (100 MHz) spectral data of compound Ang01 in $CDCl_3$

C	Ang01	
	δc, mult.[a]	δ_H, mult., *J* in Hz
1	64.6, *t*	4.83, *dt* 12.7, 1.3
		4.93, *dd*, 12.6, 1.7
2	-	-
3	165.7, s	-
4	103.5, *d*	5.28, *s*
4a	150.2, s	-
5-ax	33.9, t	2.43, *ddd*, 15.1, 10.6, 1.5
5-eq		2.61, *dd*, 15.2, 5.5
	72.7, d	4.00, *dd*, 10.4, 5.7
6	77.6, *s*	-
7	197.6, *s*	-
8	112.9, *s*	-
8a	43.8, *t*	2.34, *d*, 6.2
1′	66.1, *d*	4.08, *m*
2′	18.3, *q*	1.24, *d*, 6.5
3′	23.5, *q*	1.25, s
7-Me		

[a] Multiplicity was determined by analyses of DEPT spectra.

As well as, in part, from the biosynthetic pathway of these metabolites, supported the proposed stereochemistry of H-6 and H-7 in Ang01. It is known that the hexaketide chromophore of azaphilone pigments, e.g. Ang01 and FK17-P2b2 (Ang04), are derived from the condensation of acetate and malonate by polyketide synthase (Figure 48) while the side chain of these pigments originated from a medium-chain fatty acid synthesized via fatty acid synthetic pathway (Hajjaj et al., 2000). The azaphilone chromophore is subsequently esterified with a medium chain fatty acid to furnish the observed products as shown in Figure 48.

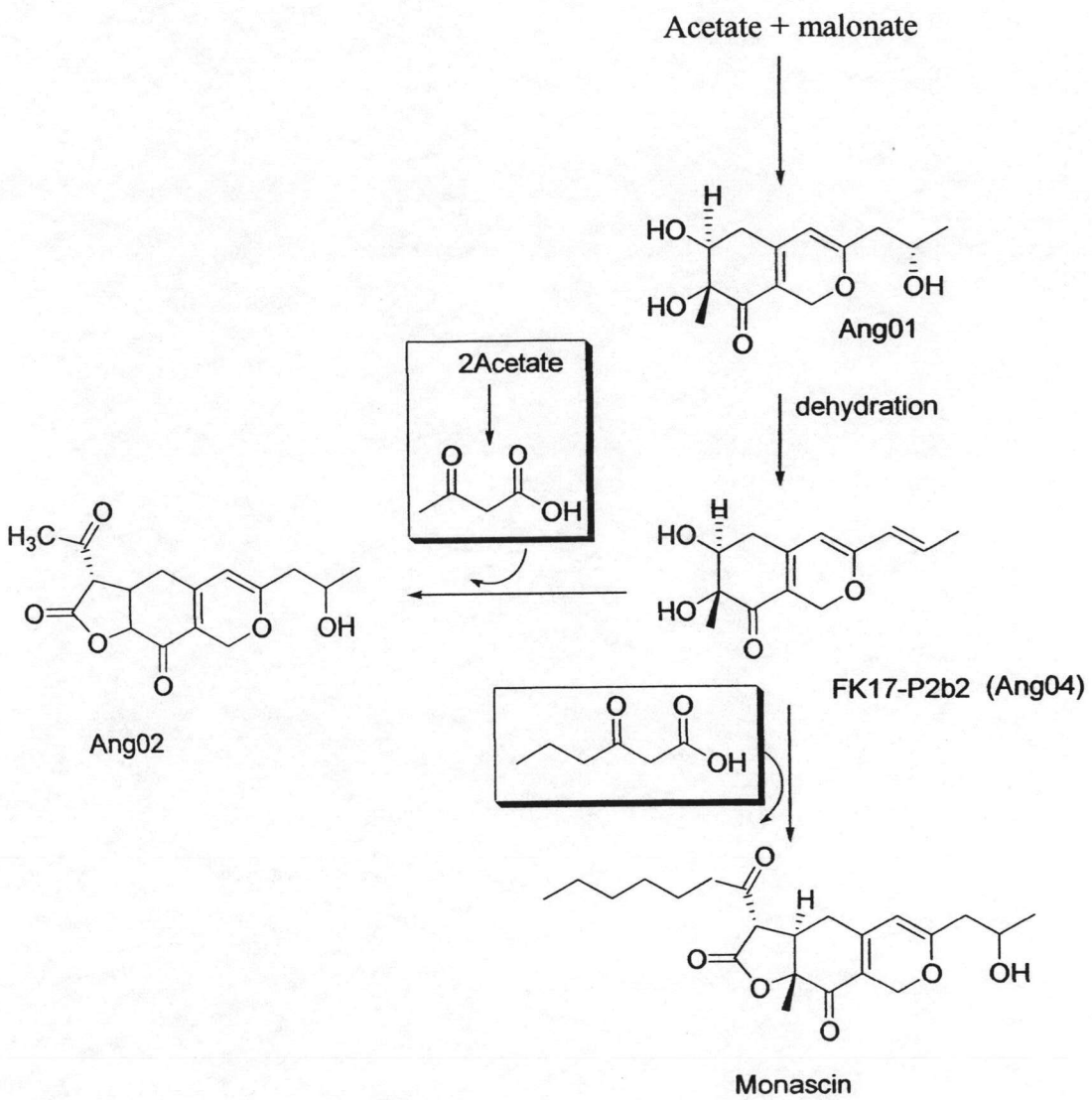

Figure 48 Possible biosynthetic pathway of azaphilone pigments Ang01-Ang04 by the fungus *M. kaoliang*

8.3 Structure Elucidation of Compound Ang02

Ang02 was obtained as yellow viscous liquid. A molecular formula $C_{17}H_{18}O_5$, [*m/z* 303.1235 $(M + H)^+$, calculated for 303.1232] was established from ESITOF mass spectrum (Figure 57). The IR absorption (Figure 56) showed OH stretching at 3447 cm^{-1}, CH stretching of alkane at ν 2927 cm^{-1}, C=O stretching at ν 1784 cm^{-1}, CH deformation of CH_2 and CH_3 ν 1380 cm^{-1}, and C-O stretching at ν 1263 cm^{-1}. The UV absorption showed λ_{max} at 243 and 375 nm (Figure 55).

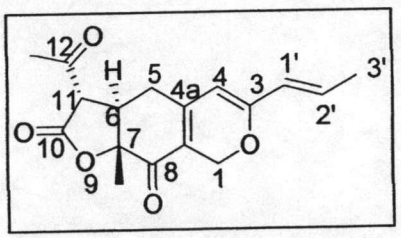

In general, the ^1H and ^{13}C NMR spectra of Ang02 were similar to those of monascin (Ang03) except that the aliphatic hydrocarbon signals of the hexoyl moiety in monascin (Ang03) were replaced by a down-field singlet methyl (δ_H 2.53 with δc 30.0) in Ang02. The ^1H NMR spectral ($CDCl_3$) (Figure 58) of compound Ang02 showed signals of three methyls at δ_H 1.5 (3H, *s*), 1.9 (3H, *dd*, *J* = 7.0, 1.5), and 2.53 (3H, *s*), a methylene of multiplet and doublet of doublet at δ_H 2.50 (1H, *m*), and δ_H 2.76 (1H, *dd*, *J* =17.6, 4.1), a methylene of doublet of doublet at δ_H 4.76 (1H, *dd*, *J* = 12.6, 1.4) and δ_H 5.11 (1H, *dd*, *J* =12.6, 1.2), three olefinic protons at δ_H 5.32 (1H, *s*), δ_H 5.95 (1H, *dd*, *J* =15.4, 1.6), and δ_H 6.56 (1H, *m*), a doublet of doublet of doublet methine δ_H 3.22 (1H, *ddd*, *J* = 17.3, 13.2, 4.1), and a doublet methine δ_H 3.70 (1H, *d*, *J* = 13.2).

The ^{13}C NMR spectrum of compound Ang02 revealed 17 signals, while DEPT 135 spectrum data (Figure 60) revealed three methyl carbons δc 17.7 (C-7Me), δc 18.5 (C-3′), and δc 30 (C-13), two methylenes δc 29.5 (C-5), δc 63.8 (C-1), five methines δc 42.8 (C-6), δc 55.6 (C-11), δc 103.3 (C-4), δc 124.4 (C-1′), and δc 135.5 (C-2′), and seven quaternary carbons δc 83.1 (C-7), δc 113.9 (C-8a), δc 150.8 (C-4a), δc 160.3 (C-3), δc 169.3 (C-10), δc 189.7 (C-8), and δc 200.2 (C-12).

The ^1H–^1H COSY spectrum (Figure 62) of compound Ang02 established the connectivity from H-1′ (δ_H 5.95) through H-3′ (δ_H 1.9) and the corrleation from H-6 (δ_H 3.22) to H-5 (δ_H 2.55 and 2.76). The HMBC (Figure 64) spectrum data of Ang02 well assembled its gross structure; key long-ranged ^1H-^{13}C corrleation were observed from H-1 (δ_H 4.76 and 5.11) to C-3 (δc 160.3), C-4a (δc 150.8), and C-8a (δc 113.9); H-4 (δ_H 5.32) to C-3, C-5 (δc 29.5), C-8a and C-1′ (δc

124.4); H-5 (δ_H 2.5) to C-8a; 7-Me protons (δ_H 1.50) to C-6 (δc 42.8), C-7 (δc 83.1), and C-8 (δc 189.7); H-11 (δ_H 3.7) to C-6, C-10 (δc 169.3), and C-12 (δc 200.2); H-13 (δ_H 2.49) to C-12; and both H-1′ (δ_H 5.95) and H-2′ (δ_H 6.50) to C-3′. Based upon these spectral data, the structure of Ang02 was established as shown. Ang02 exhibited a positive optical rotation similar to that of monascin (Ang03) implying that Ang02 possessed the same stereochemistry as that of monascin (Ang03).

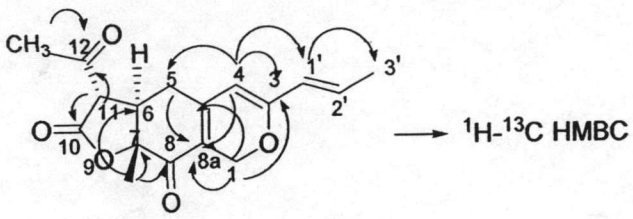

Table 22 The ^{1}H (400 MHz) and ^{13}C NMR (100 MHz) spectral data of compound Ang02 in $CDCl_3$

C	Ang02	
	δc, mult.[a]	δ_H, mult., J in Hz
1	63.8, *t*	4.76, *dd*, 12.6, 1.4
		5.11, *dd*, 12.6, 1.2
2	-	-
3	160.3, *s*	-
4	103.3, *d*	5.32, *s*
4a	150.8, *s*	-
5	29.5, *t*	2.50, *m*
		2.76, *dd*, 17.6, 4.1
6	42.8, *d*	3.22, *ddd*, 17.3, 13.2, 4.1
7	83.1, s	-
8	189.7, *s*	-
8a	113.9, *s*	-
9	-	-
10	169.3, *s*	-
11	55.6, *d*	3.70, *d*, 13.2
12	200.2, *s*	-
13	30.0, *q*	2.53, *s*

C	Ang02	
	δc, mult.[a]	δ_H, mult., J in Hz
1′	124.4, *d*	5.95, *dd*, 15.4, 1.6
2′	135.5, *d*	6.56, *m*
3′	18.5, *q*	1.90, *dd*, 7.0, 1.5
7-Me	17.7,*q*	1.50, *s*

[a] Multiplicity was determined by analyses of DEPT spectra.

Structure Elucidation of Compound Ang03

A compound Ang03 was obtained as yellow crystal. Ang03 possessed a molecular formula $C_{21}H_{26}O_5$, as deduced from the ESI mass spectrum, showing a prominent peak [*m/z* 381.55 $(M + Na)^+$] (Figure 71). The UV absorption showed λ_{max} at 243 and 373 nm (Figure 70).

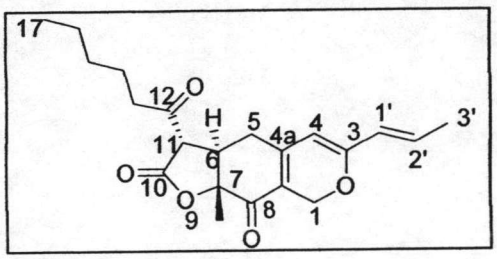

The ^{1}H NMR spectrum ($CDCl_3$) (Figure 72) of compound Ang03 showed signals of three methyls at δ_H 0.92 (3H, t), 1.50 (3H, s), and 1.92 (3H, *dd*, *J* =7.0, 2.0), three methylene of multipletes at δ_H 1.38-1.7(1H, *m*), three non equivalent of methylene groups at δ_H 2.48 (1H, m), 2.69 (1H, *dd*, *J* = 17.6, 5.9), δ_H 4.77 (1H, *dd*, *J* = 12.5, 1.4), and δ_H 5.12 (1H, *dd*, *J* = 11.7, 0.9), a methylene of doublet of doublet of doublet at δ_H 2.69 (1H, *m*), and δ_H 3.08 (1H, *ddd*, *J* = 18.1, 7.2, 3.6), three olefinic protons at δ_H 5.32 (1H, s), δ_H 5.91 (1H, *dd*, *J* = 15.3, 1.6), and δ_H 6.54 (1H, *m*), a doublet of doublet of doublet methine δ_H 3.28 (1H, *ddd*, *J* = 15.8, 11.7, 4.1), and a methine doublet δ_H 3.72 (1H, *d*, *J* = 13.3).

The ^{13}C NMR spectrum of compound Ang03 revealed 21 signals, while DEPT 135 spectrum data (Figure 74) revealed three methyl carbons δc 13.9 (C17), δc 17.7 (C-3′), and δc 18.5 (C-7Me), six methylene carbons δc 22.8 (C-16), δc 31.2 (C-15), δc 29.7 (C-5), δc 42.9 (C-13), δc 22.2 (C-14), and δc 63.8 (C-1), five methines δc 43.1 (C-6), δc 54.9 (C-11), δc 103.3 (C-

4), δc 124.4 (C-1′), and δc 135.5 (C-2′), and seven quaternary carbons δc 83.2 (C-7), δc 114.0 (C-8a), δc 150.8 (C-4a), δc 160.7 (C-3), δc 169.5 (C-10), δc 189.5 (C-8), and δc 202.5 (C-12).

• The ^{1}H–^{1}H COSY spectrum (Figure 76) of compound Ang03 displayed the connectivity from H-1′ (δ_H 5.91) through H-3′ (δ_H 1.92) and the corrleation from H-5 (δ_H 2.48 and 2.69) to H-11 (δ_H 3.72) and H-14 to H-17. The HMBC (Figure 77) spectrum data of Ang03 demonstrated long-ranged ^{1}H-^{13}C corrleation of Ang03 from H-1 (δ_H 4.77 and 5.12) to C-3 (δc 160.7), C-4a (δc 150.8), and C-8a (δc 114.0); H-4 (δ_H 5.32) to C-3, C-5 (δc 29.7), C-8a (114.0) and C-1′ (δc 124.4); H-5 (δ_H 2.48, 2.69) to C-8a; 7-Me protons (δ_H 1.50) to C-6 (δc 43.1), C-7 (δc 83.2), and C-8 (δc 189.5); H-11 (δ_H 3.72) to C-6, C-10 (δc 169.5), and C-12 (δc 202.0); H-13 (δ_H 2.50) to C-12, to C-14 (δc 31.2), and C-15 (δc 22.8); and both H-1′ (δ_H 5.91) and H-2′ (δ_H 6.54) to C-3 and C3′.

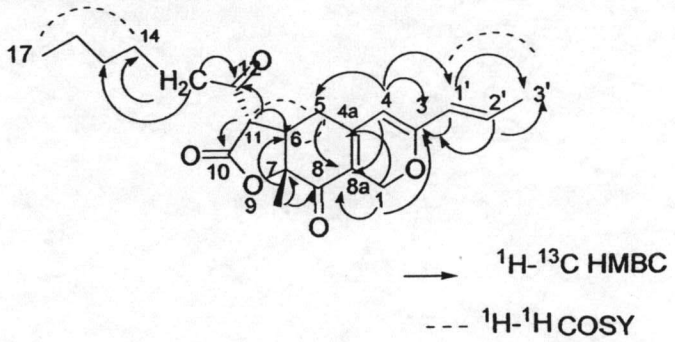

Combination of the fragments mentioned above led to assignment of structure of Ang03. Therefore compound Ang03 was identified as monascin which is a known substance previously isolated from *M. purpureus* (Chen *et al.*, 1971). Assignment of protons and carbons of Ang03 is in Table 23.

Table 23 Comparison of ^{1}H and ^{13}C NMR spectral data of compound Ang03 and monascin in $CDCl_3$

C	Ang03		Monascin
	δc, mult.[a]	δ_H, mult., J in Hz	δ_H, mult., J in Hz
1	63.8, *t*	4.77, *dd*, 12.5 1.4	4.76, *q* 12.6
		5.12, *dd*, 11.7, 0.9	5.06, *q*, 12.6
2	-	-	-
3	160.7, *s*	-	-
4	103.3, *d*	5.32, *s*	5.32, *s*
4a	150.8, *s*	-	-
5	29.7, t	2.48, *m*	2.6, *m*
		2.69, *m*	
6	43.1 *d*	3.28, *ddd*, 15.8, 11.7, 4.1	3.3, *q*, 8.3, 5
7	83.2, *s*	-	-
8	189.5, *s*	-	-
8a	114.0, *s*	-	-
9	-	-	-
10	169.5, *s*	-	-
11	54.9, *d*	3.72, *d*, 13.3	3.75, *d*, 13.0
12	202.5, *s*	-	-
13	42.9, *t*	3.08, *m*	3.08, *m*
		2.69, *m*	2.69, *m*
14	22.2, *t*	1.65, *m*	1.65, *m*
15	31.2, *t*	1.38, *m*	1.45, *m*
16	22.8, *t*	1.7, *m*	1.7, *m*
17	13.9, *q*	0.92, *t*,	0.95
1′	124.4, *d*	5.91, *dd*, 15.3, 1.6	5.96, *d*, 15.6
2′	135.5, *d*	6.54, *m*	6.58
3′	17.7, *q*	1.92, *dd*, 7.0, 2.0	1.88, *d*, 6.8
7-Me	18.5, *q*	1.50, *s*	1.50, *s*

[a] Multiplicity was determined by analyses of DEPT spectra.

8.4 Structure Elucidation of Compound Ang04

Compound Ang04 was obtained as yellow viscous liquid. Ang04 possessed a molecular formula $C_{13}H_{16}O_4$ as revealed by the ESITOF mass spectrum (Figure 81), showing a prominent peak at [m/z 259.0943 $(M + Na)^+$, calculated for 259.0946]. The IR spectrum displayed OH stretching 3364 cm^{-1}, and C=O stretching at ν 1715 cm^{-1} (Figure 80). The UV absorption showed λ_{max} at 245 and 349 nm (Figure 79).

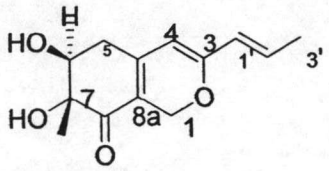

The ^{1}H-NMR spectral ($CDCl_3$) data of compound Ang04 (Figure 82) displayed signals of two methyls (as a singlet and a doublet) at δ_H 1.25 (3H) and 1.89 (3H, *d*, J = 6.5), two non equivalent methylene groups at δ_H 2.50 (1H, *ddd*, *J* =18.1, 10.8, 1.5), δ_H 2.67 (1H, *dd*, *J* =18.2, 4.0) and δ_H 4.83 (1H, *dd*, *J* =12.8, 1.4), δ_H 4.92 (1H, *dd*, *J* =12.5, 1.6), a singlet olefinic proton (at δ_H 5.28), a doublet of doublet olefenic δ_H 5.94 (1H, *dd*, *J* =15.4, 1.7), a methine δ_H 4.05 (1H, *dd*, *J* =10.7, 5.5) and an olefenic multiplet δ_H 6.51.

In general, the ^{1}H and ^{13}C NMR spectra of Ang04 were similar to those of Ang01, except that the oxygenated methine and doublet methylene protons signals of propyl moiety in Ang01 were replaced by olefenic hydrocarbon signals (δ_H 5.94 and δ_H 6.51) in Ang04. The HMQC spectral data of Ang04 (Figure 84) was assisted in the assignment of protons attached to their corresponding carbons (Table 24). Attachment of the unsaturated sp^2 C-3 to an oxygen atom in Ang04 was evident from a downfield shift of its ^{13}C resonance (at δc 160.8).

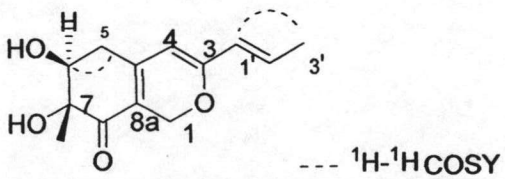

The ^{1}H–^{1}H COSY spectrum (Figure 85) of compound Ang04 established the connectivity from H-1′ (δ_H 5.94) through H-3′ (δ_H 1.89) and the coupling between H-6 (δ_H 4.05) and H-5 (δ_H 2.50 and 2.67). The HMBC spectrum showed correlations from H-1 (δ_H 4.83 and 4.92) to C-3 (δc 160.8), C-4a δc 150.5), and C-8a (δc 112.9); H-4 (δ_H 5.28) to C-3, C-5 (δc

33.7), and C-1′; H-5 (δ_H 2.50 and 2.67) to C-4a and C-8a; 7-Me protons (δ_H 1.25) to C-6 (δc 72.7), C-7 (δc 76.8), and C-8 (δc 196.9); H-1′ to C-3 and C-1′ (δc 124.6); H-2′ (6.51) to C-3; H-3′ to C-1′ and C-2′. Combination of the fragment mentioned above led to assignment of structure of Ang04 (Table 24). Therefore compound Ang04 was identified as FK17-P2b2, which is a known substance, previously isolated from *Aspregillus* sp. (Takayuki and Hiroshi, 1994).

Table 24 The ^{1}H (400 MHz) and ^{13}C NMR (100 MHz) spectral data of compound Ang04 in $CDCl_3$

C	Ang04	
	δc, mult.[a]	δ_H, mult., J in Hz
1	64.0, *t*	4.83, *dd* ,12.8, 1.4
		4.92, *dd*, 12.5, 1.6
2	-	-
3	160.8, *s*	-
4	103.4, *d*	5. 28, *s*
4a	150.5, *s*	-
5	33.7, *t*	2.50, *ddd*, 18.1, 10.8, 1.5
		2.67, *dd*, 18.2, 4.0
6	72.7, *d*	4.05, *dd*, 10.7, 5.5
7	76.8, *s*	-
8	196.9, *s*	-
8a	112.9, *s*	-
1′	124.6, *t*	5.94, *dd*, 15.4, 1.7
2′	135.2, *d*	6.51, *m*
3′	18.5, *q*	1.89, *d*, 6.5
7-Me	18.1, *q*	1.25, *s*

[a] Multiplicity was determined by analyses of DEPT spectra.

Ang01, the major metabolite of *M. kaoliang* KB20M10.2, was inactive against the malarial parasite (*Plasmodium falciparum*), *Mycobacterium tuberculosis* H37Ra, and *Candida albicans*. Compound Ang01 showed no cytotoxicity against BC (breast cancer) and KB (human epidermoid carcinoma of cavity) cell lines. Unfortunately, due to the limited amount of materials, the minor metabolites, compounds Ang02, Ang03, and Ang04, were not tested for their biological activities. A previous study reported that monascin (Ang03) and its derivatives possessed mild antibiotic activity against *Bacillus subtilis* and *Candida pseudotropicalis*, and also showed immunosuppressive activity on mouse T-splenocytes (Martinkova *et al.*, 1999). Results from this present investigation and from that reported by Martinkova *et al.* (1999) confirmed that monascin (Ang03) and its derivatives are not toxic, and this may be the reason why pigments of the *Monascus* species have been widely used as natural food colorant in East Asia since ancient times particularly for Chinese food and cosmetics. FK17-P2b2 (Ang04) was previously patented as a novel UV-absorbing compound, and its excellent near ultraviolet region absorbing ability is very useful for protecting various kinds of industrial products from deterioration and can be used as an additive in cosmetics (Takayuki and Hiroshi, 1994).

9. Physical and chemical properties of the isolated compounds

9.1 PNK01

Compound PNK01 was obtained as orange yellow amorphous powder, soluble in $CHCl_3$ (53.0 mg, 3.53 % based on the ethyl acetate extract).

$[\alpha]^{25}_{D}$	:+48.21 $^{\circ}$ (0.50, $CHCl_3$)
UV	: λ_{max} nm ($\in$) in $CHCl_3$; Figure 22
	at 262 (10005), 307 (11835) nm
IR	: ν_{max} cm^{-1}; Figure 23
	3751, 3442, 3200, 2929, 1735, 1655, 1510, 880
ESITOFMS	: *m/z*; Figure 24
	583.2637 $(M + Na)^+$
^{1}H-NMR	: δ_H (ppm), 400 MHz, in $CDCl_3$
	See Figure 25 and Table 20
^{13}C-NMR	: δc (ppm), 100 MHz, in $CDCl_3$
	See Figure 28 and Table 20

9.2 Ang01

Ang01 was obtained as yellow viscous liquid, soluble in $CHCl_3$ (80 mg, 8.0×10^{-3}% based on the fermented rice).

$[\alpha]^{25}_D$	:+71.95° (0.23, $CHCl_3$)
UV	: λ_{max} nm ($\in$) in $CHCl_3$; Figure 35
	at 243 (4286), 346 (4765) nm
IR	: ν_{max} cm^{-1}; Figure 36
	3350, 2974, 1650, 1554, 1409, 1290, 1193, 978
ESITOFMS	: *m/z*; Figure 37
	277.1041 $(M + Na)^+$
^{1}H-NMR	: δ_H (ppm), 400 MHz, in $CDCl_3$
	See Figure 38 and Table 21
^{13}C-NMR	: δc (ppm), 100 MHz, in $CDCl_3$
	See Figure 40 and Table 21

9.3 Ang02

Ang02 was obtained as yellow viscous liquid, soluble in $CHCl_3$ (2.8 mg, 2.8×10^{-4}% based on the fermented rice).

$[\alpha]^{25}_D$	:+205.5° (0.28, $CHCl_3$)
	at 243 (5121), 375 (4822) nm
IR	: ν_{max} cm^{-1}; Figure 56
	3447, 2927, 1791, 1380, 1784, 1526, 1380, 1263
ESITOFMS	: *m/z*; Figure 57
	303.1235 $(M + H)^+$
^{1}H-NMR	: δ_H (ppm), 400 MHz, in $CDCl_3$
	See Figure 58 and Table 22
^{13}C-NMR	: δc (ppm), 100 MHz, in $CDCl_3$
	See Figure 60 and Table 22

9.4 Ang03

Ang03 was obtained as yellow crystal, soluble in $CHCl_3$ (20 mg, 2.0 x 10^{-3}% based on the fermented rice).

$[\alpha]^{25}_D$	:+255.25° (0.23, $CHCl_3$)
UV	: λ_{max} nm (ϵ) in $CHCl_3$; Figure 70
	at 246(4875), 373 (5387) nm
IR	: ν_{max} cm^{-1}
	2974, 1709, 1656
ESITOFMS	: *m/z*; Figure 71
	381.55 $(M + Na)^+$
^{1}H-NMR	: δ_H (ppm), 400 MHz, in $CDCl_3$
	See Figure72 and Table 23
^{13}C-NMR	: δc (ppm), 100 MHz, in $CDCl_3$
	See Figure 74 and Table 23

9.5 Ang04

Ang04 was obtained as yellow viscous liquid, soluble in $CHCl_3$ (4.2 mg, 4.2 x 10^{-4}% based on the fermented rice).

$[\alpha]^{25}_D$	:+85.14° (0.23, $CHCl_3$)
UV	: λ_{max} nm (ϵ) in $CHCl_3$; Figure 79
	at 245 (4286), 350 (4765) nm
IR	: ν_{max} cm^{-1}; Figure 80
	: 3350, 2974, 1714, 1554, 1451, 1380, 1180, 1083
ESITOFMS	: *m/z*; Figure 81
	259.10 $(M + Na)^+$
^{1}H-NMR	: δ_H (ppm), 400 MHz, in $CDCl_3$
	See Figure 82 and Table 24
^{13}C-NMR	: δc (ppm), 100 MHz, in $CDCl_3$
	See Figure83 and Table 24